Fisheries New Zealand

Tini a Tangaroa

Acoustic estimates of southern blue whiting from the Campbell Island Rise, August-September 2022 (TAN2210)

New Zealand Fisheries Assessment Report 2023/37

P.C. Escobar-Flores,
Y. Ladroit,
S. Holmes

ISSN 1179-5352 (online)
ISBN 978-1-991087-39-3 (online)

August 2023

Te Kāwanatanga o Aotearoa
New Zealand Government

Disclaimer

Requests for further copies should be directed to:

Fisheries Science Editor
Fisheries New Zealand
Ministry for Primary Industries
PO Box 2526
Wellington 6140
NEW ZEALAND

Email: Fisheries-Science.Editor@mpi.govt.nz
Telephone: 0800 00 83 33

This publication is also available on the Ministry for Primary Industries websites at:
http://www.mpi.govt.nz/news-and-resources/publications
http://fs.fish.govt.nz go to Document library/Research reports

Please cite this report as:

Escobar-Flores, P.C.; Ladroit, Y.; Holmes, S. (2023). Acoustic estimates of southern blue whiting from the Campbell Island Rise, August-September 2022 (TAN2210). *New Zealand Fisheries Assessment Report 2023/37.* 58 p.

TABLE OF CONTENTS

EXECUTIVE SUMMARY

Escobar-Flores, P.C.[1]; Ladroit, Y.[1]; Holmes, S[1]. (2023). Acoustic estimates of southern blue whiting from the Campbell Island Rise, August-September 2022 (TAN2210).

***New Zealand Fisheries Assessment Report 2023/37.* 58 p.**

The 14th acoustic survey to evaluate the biomass of the southern blue whiting stock (SBW) off Campbell Island (SBW 6I) was carried out onboard RV *Tangaroa* between 28 August and 23 September 2022. Two acoustic snapshots were successfully completed using the NIWA dual frequency towed body (DuFT) as the primary acoustic system.

Thirteen strata were surveyed during snapshot 1 between 30 August and September 11, including a new stratum northwest of Campbell Island (stratum 11), defined to encompass the extended fishing effort in 2021. Strata definitions for snapshot 2 were modified according to the distribution of SBW observed during snapshot 1 and the distribution of the commercial fleet; 10 strata, covering a smaller survey area, were surveyed between 12 and 20 September 2022. An aggregation-based snapshot was also carried out during snapshot 2 at the eastern boundary of the survey area (stratum 12) to survey a spawning aggregation of SBW. Maturity data showed that snapshot 1 was carried out between spawning events, and that snapshot 2 was carried out while adult SBW were actively spawning.

Twelve research mark identification trawls were completed during the survey. During snapshot 1, five bottom trawls targeted juvenile (n = 3) and adult (n = 2) SBW marks. During snapshot 2 seven trawls were completed: three bottom trawls targeted adult (n = 1) and juvenile (n = 2) SBW marks; and four midwater trawls targeted adult (n = 2) and juvenile (n = 2) marks. Poor weather reduced the number of research mark identification trawls completed during the survey.

Pre-spawning aggregations of adult SBW were found in the northern (stratum 2) area of the survey in the snapshot 1, and in the southern area of the survey (stratum 7S) in snapshots 1 and 2. A spawning aggregation of adult SBW was observed at the eastern boundary of stratum 8 during snapshot 2. Average lengths of adult SBW from the eastern area in both commercial and research trawls were about 5 cm larger than those from the northern and southern areas. Commercial length frequency data were used to convert acoustic densities to biomass for adult SBW.

The estimates of biomass of adult SBW in 2022 were 87 919 t (CV 26%) in snapshot 1 and 96 016 t (CV 29%) in snapshot 2, resulting in an average estimate of 91 968 t (CV 20%). This was slightly higher (< 1%) than the equivalent adult estimate from 2019 (91 145 t, CV 27%). The average estimate of biomass for immature SBW in 2022 was 5356 t (CV 22%), which was 27% higher than in 2019 (4060 t, CV 18%). The average estimate of biomass of juvenile SBW in 2022 was 12 764 t (CV 14%) and was the highest in the time series. The high biomass of juvenile SBW in 2022 was due to extensive juvenile marks in the shallow areas in the northern (e.g., 2, 4, and 5) and southern strata (e.g., 7N) in both snapshots.

[1] National Institute of Water and Atmospheric Research (NIWA), New Zealand.

1. INTRODUCTION

Southern blue whiting (*Micromesistius australis*) is one of New Zealand's largest volume fisheries, with annual landings of between 13 000 t and 42 000 t for 2000–2022 (Fisheries New Zealand 2022). Southern blue whiting (SBW) occur mainly in Sub-Antarctic waters. Four stocks in FMA 6 are defined based on their known spawning grounds: Bounty Platform (SBW 6B); Pukaki Rise (SBW 6R); Auckland Islands Shelf (SBW 6A); and Campbell Island Rise (SBW 6I) (Figure 1).

The Campbell Island Rise stock is the largest of the four SBW stocks. Catch limits with area-specific sub-limits were introduced in 1992–93. With the introduction of SBW into the Quota Management System (QMS) on 1 November 1999, separate total allowable commercial catches (TACCs) for each of the four main stocks in FMA 6 were set (Fisheries New Zealand 2021). From 1 April 2014 the TACC for SBW 6I was set at 39 200 t, but catches have been below the level of the TACC since, with a catch of only 12 000 t in 2021 (Fisheries New Zealand 2022).

Spawning of SBW occurs on the Campbell Plateau from late August to late September (Large et al. 2021). During spawning, SBW typically form large midwater aggregations. Commercial and research fishing on spawning SBW aggregations result in very clean catches of SBW (about 90% in research trawls in 2019 (Ladroit et al. 2020b)). The occurrence of single-species spawning aggregations allows accurate biomass estimation using acoustics.

A time series of acoustic surveys for SBW on the Campbell Plateau was started in 1993 (Hanchet & Haist 1994). These area-based acoustic surveys are used to measure relative abundance of adult SBW and to predict pre-recruit numbers, and they have been important inputs into the stock assessment for the last 20 years (e.g., Doonan 2020). The movement of fish during the survey period required the development of an adaptive survey design to increase efficiency (Dunn & Hanchet 1998, Dunn et al. 2001). There have been 13 surveys of the Campbell grounds (1993, 1994, 1995, 1998, 2000, 2002, 2004, 2006, 2009, 2011, 2013, 2016, and 2019), all of them carried out from research vessel (RV) *Tangaroa* using towed systems as the primary acoustic instrument and hull systems as the secondary instrument (all 38 kHz).

Biomass estimates of adult SBW from the two most recent surveys in 2016 (O'Driscoll et al. 2018) and 2019 (Ladroit et al. 2020b) were relatively high due to recruitment of the above-average 2009, 2011, 2014, and 2015 year classes into the fishery. The estimated abundance of immature SBW in 2019 was below average for the time series (Ladroit et al. 2020b); this suggests that the 2016 and 2017 year classes (ages three and two, respectively, in 2019) were not abundant.

As SBW recruit at two and three years to the fishery (Hanchet 1993), surveys are currently scheduled every three years to provide up-to-date indices for the stock assessment. The survey in 2022 was the 14th in the time series and it consisted of two acoustic snapshots (sub-surveys) conducted between 26 August and 23 September.

This report fulfils the final reporting requirement of Fisheries New Zealand research project SBW2021-01. The overall objective was to estimate the biomass of southern blue whiting (*Micromesistius australis*) on the Campbell Plateau (SBW 6I) using acoustic surveys.

The specific objectives of this project were:

1. To estimate pre-recruit and spawning biomass on the Campbell Plateau using an acoustic survey, with a target coefficient of variation (CV) of the estimate of 30%.
2. To calibrate acoustic equipment used during the survey.

2. METHODS

2.1 Survey design

The time series of acoustic estimates for the Campbell Island Rise SBW stock are from area-based surveys. The area of the survey is defined based on historical and recent fishing effort, past surveys, and the known distribution range of the SBW stock off Campbell Island. The survey area typically extends from the 300 m depth contour in the west to the eastern and southern boundaries of the Campbell Plateau, which varies in depth from about 480 to 750 m.

These surveys provide fishery independent monitoring of the recruited part of the population as well as predicting the strength of year classes about to enter the fishery.

An aggregation-based survey design is not appropriate for this fishery. Although much of the adult spawning biomass may be concentrated in one or more localised aggregations, a variable proportion of the biomass occurs away from these aggregations. Attempts have been made to survey the main SBW spawning aggregations on the Campbell Island Rise from industry vessels in 2003 (O'Driscoll & Hanchet 2004) and 2006 (O'Driscoll et al. 2006), but these gave much lower estimates of SBW biomass than those obtained from wide-area surveys. For example, the aggregation-based survey by two industry vessels in 2006 gave estimates of abundance that were only 10–15% of those from the wide-area research survey in the same year (O'Driscoll et al. 2006, O'Driscoll et al. 2007). The acoustic survey design presented here also provides an abundance estimate of pre-recruit SBW, which typically occur outside the area being fished by the commercial fleet (i.e., away from the main aggregations).

The most suitable time for an acoustic survey of SBW is when they aggregate to spawn at the beginning of the austral spring. On the Campbell Island Rise, the onset of spawning has been typically observed between 6 and 17 September (range 3–20 September) (Large et al. 2021).

The 2022 survey was carried out from 26 August to 23 September 2022 to maximise the chances of covering the spawning period. The 29-day booking of RV *Tangaroa* allowed for 21 days in the survey area, 1 day for acoustic calibration, 2 days for mobilisation and demobilisation of equipment to and from RV *Tangaroa*, and 5 days steaming to and from Wellington.

The study aimed to carry out at least two acoustic snapshots (i.e., complete set of transects allocated to cover a survey area) of the Campbell Island Rise spawning area with an overall target CV of 30% (as specified by the project objectives). The survey followed the two-phase design recommended by Dunn & Hanchet (1998) and Dunn et al. (2001), incorporating the modifications recommended by Hanchet et al. (2003).

Stratum boundaries were re-evaluated before the survey by examining the location of the commercial fishing fleet up to and including 2021. The location of the commercial catch has varied considerably over time (Figure 2). While a high proportion of the catch was consistently taken from the core survey area over the last six years (strata 2–7 in Figure 2), some catch was taken east of the core area in 2016 and 2018, and west of the northern strata (stratum 2) outside the core survey area in 2021.

Although almost all of the commercial catch and effort between 2016 and 2020 (see Figure 2) was within the stratum boundaries of the 2016 and 2019 surveys, which included eastern areas, about 25% of the commercial catch from 2021 was taken from an area to the northwest of these boundaries. Therefore, we proposed a stratification for 2022 that retained the 2016 and 2019 stratum boundaries, with the addition of a new stratum (stratum 11) west of stratum 2 (see Figure 3).

As in all previous surveys, the parallel transect approach of Jolly & Hampton (1990) was used. Transect locations were randomly generated and were carried out at right angles to the depth contours (i.e., from shallow to deep or vice versa). The minimum distance between transect midpoints varied between strata and was calculated as follows:

$$m = 0.5\ L/n \qquad (1)$$

where m is the minimum spacing distance in nautical miles, L is the length of the stratum in nautical miles, and n is the number of transects. The proposed transect allocation for snapshot 1 is available in Table 1.

Because of the highly aggregated nature of spawning SBW, additional adaptive phases are considered appropriate to reduce the CVs of the biomass estimates. These adaptations include: allowing for up to 20% of transects to be assigned to a second phase; adding additional aggregation snapshots; and using information from the location of the fleet on the distribution of the fish at the time of the survey to refine strata boundaries and/or add strata. Information from snapshot 1 is typically used to redefine the survey strata and the associated sampling effort for snapshot 2.

During snapshot 1 aggregations of adult SBW were detected in the northern and southern area of the survey in strata 2 and 7S. No aggregations of adult SBW were detected in the eastern strata (i.e., 6 and 8). The proposed survey design was modified during snapshot 1 in two ways:

1. Stratum 6S was reduced. Because of time constrains and the absence of fish aggregations in the northern two transects of stratum 6S and on the eastern transects of stratum 7S, the southernmost transect in stratum 6S (transect #3) was not completed. Stratum 6S was therefore shortened with the new southern boundary defined at 53° 12’ S.
2. The boundaries of stratum 7S were modified by shifting it to the west. A large midwater pre-spawning aggregation of adult SBW was found across several transects in stratum 7S including the westernmost transect of the stratum (transect #1), and the western boundary of the stratum was therefore extended to 169° 10’ E following the 300 m depth contour, and a new transect (#9) was added. The acoustic density of the aggregations in 7S decreased from west to east and transect #5 had no aggregations of SBW. To make the best use of the time available, the eastern extent of stratum 7S was reduced to 170° 20’ E. Therefore, transect #5 became the zero bounding transect for the stratum, and the total number of transects for the stratum was 6 instead of the 8 transects initially proposed.

The final stratum definition and transects completed during the snapshot 1 are shown in Figure 4.

The transect allocation for the second snapshot was determined based on the fish densities observed in snapshot 1, the location of the fleet, and the remaining survey time. Snapshot 2 was largely based on snapshot 1; however the number of strata and survey area were decreased due to time constraints. The final stratum definition for snapshot 2 are given below.

1. Stratum boundaries from snapshot 1 were used for strata 11, 2, 3S, 5, and 7N.
2. The area of stratum 7S was further reduced at its southern end to 53° 30’ S.
3. Strata 6N and 6S were combined into a new stratum 6, with a new southern boundary defined at 52° 40’ S (the same southern boundary as stratum 8S and 8E in snapshot 1).
4. Strata 8N, 8S, and 8E were combined into a single stratum 8, which was reduced on its eastern boundary to 171° 50’ E.
5. Stratum 3N was not included in snapshot 2.
6. A new stratum (#12) was added. Following an adaptive survey design, an aggregation-based snapshot was used to survey midwater aggregations attributed to adult SBW at the eastern edge of stratum 8 around 52° 18’ S.

The final stratum definitions and transects for snapshot 2 are shown in Figure 5 and summary data are given in Table 2.

2.2 Acoustic data collection

NIWA’s dual frequency towed body (DuFT) was the primary acoustic instrument used to collect acoustic data for biomass estimation during the survey. The DuFT was towed using a cable which has a fibre link, allowing for the data to be seen and quality-controlled in real time during the acquisition from the vessel's acoustic lab. The instrument was powered using a lithium battery. Acoustic data were collected at 38 and 120 kHz using a Simrad wide-band transceiver (WBT) tube. The software used for data acquisition was the EK80 version 21.15.1.

Acoustic data were also continuously collected acoustic data using the five-frequency hull system on RV *Tangaroa* (18, 38, 70, 120, and 200 kHz); however the 38 and 120 kHz were in passive mode while the vessel was in survey mode (i.e., DuFT deployed for data collection). The echosounder settings used during the survey in both systems are shown in Table 3.

Calibrations of the hull mounted Simrad EK80 echosounder systems on RV *Tangaroa* and DuFT took place north of Banks Peninsula (43° 12.35' S, 172° 01.63' E), at the start of the acoustic survey on 28 August 2022. The calibrations were conducted broadly as per the procedures given by Demer et al. (2015). The calibration reports are provided as Appendix 1. The calibrations were of excellent quality and indicated that the echosounders were functioning correctly, with estimated calibration parameters similar to those from previous calibrations.

2.3 Mark identification trawling

Although acoustic marks of SBW tend to be largely monospecific, problems have been encountered in the separation of pre-recruit from adult fish and the separation of pre-recruit fish from other species (Grimes & Hanchet 1999, McClatchie et al. 2000, Hanchet et al. 2003) . Mark identification trawling was therefore required as part of the acoustic survey. Likewise, because the survey around Campbell Island typically covers a wider area than that commercially fished (see Figure 2), mark identification provided complementary biological information that might not be available from observers.

Mark identification fishing aimed at:

- Establishing species mix proportions away from dominant heavy marks, which are easily identified as SBW.
- Distinguishing less dense adults marks from pre-recruit marks in areas where they occur in similar depths.
- Identifying the size and age composition of SBW in the less dense pre-recruit marks including 1, 2, and immature 3 year old fish.
- Separating the small schooling mesopelagic fish, such as the common lanternfish (*Lampanyctodes hectoris*) and pearlside (*Maurolicus australis*), from the moderately dense schools of pre-recruit SBW when they are in the shallower part of their depth range and/or close to the bottom.

Mark identification trawls were conducted using midwater and demersal trawls. Midwater marks were targeted with NIWA's fine-mesh midwater trawl which has a 13 m diameter opening and a 10 mm codend. Demersal marks were targeted using the ratcatcher wing trawl, with 50 m sweeps, 50 m bridles, and a 40 mm mesh codend.

The catch from each tow was sorted, if possible, into species level and weighed on Marel motion-compensating electronic scales accurate to about 0.1 kg. Length and biological information were recorded for a sample of SBW and other important species. Samples of up to 200 SBW and 50–200 of other species were randomly selected from the catch to measure length, sex, and gonad stage. At least 20 SBW from each tow were selected for more detailed biological analysis, which included length, fish weight, sex, gonad stage, gonad weight, and stomach state, condition, and contents. Otoliths were collected from SBW in the detailed biological sample to augment otoliths collected by the scientific observer programme. Catch data were error-checked and loaded onto the Fisheries New Zealand *trawl* database.

Scaled length frequencies of SBW from research trawls were constructed by scaling length frequencies from individual tows by the SBW catch in the tow.

Unusual or unidentified organisms were inventoried and then preserved (by freezing) for identification ashore (under Fisheries New Zealand contract BEN2021-03or for protected corals, under Department of Conservation Project DOC20303/INT2019-04).

2.4 Other data collection

A Seabird SM-37 Microcat CTD datalogger (serial number 2958) was mounted on the headline of the demersal trawl net to collect salinity and temperature data to determine the absorption coefficient and speed of sound. An RBR data logger (RBR*duet*, serial number 82704) was attached on midwater trawls to collect temperature data.

2.5 Commercial catch data

Biological information of SBW was collected by scientific observers onboard industry vessels operating in the survey area in the 2022 fishing season. The sampling of the commercial catch provided fishery-dependent data on fish size and spawning state of SBW. These data were used to calculate scaled length frequency distributions (calculated as the weighted (by catch) average of individual length samples), which were used to convert acoustic data into biomass for the adult fraction of the stock (see Section 2.7).

Observer data from the 2022 fishery were extracted from the Fisheries New Zealand Centralised Observer Database (*cod*) database on 11 November 2022.

2.6 Acoustic data analysis

Acoustic data collected during the survey were analysed using NIWA's open-source software ESP3 version 1.47.0 (Ladroit et al. 2020a). Data were visually inspected and groomed, using a combination of automated algorithms and manual editing. The grooming included: identifying and excluding from the analysis artefacts and noise (e.g., double bottom echoes, interference by other acoustic system, etc.), bottom definition (i.e., creating a bottom line across consecutive pings at a range where the acoustic samples are affected by the bottom echo), and removing bad transmits (i.e., entire pings where the acoustic signal has been attenuated due to aeration or other process becoming unusable for analysis).

Acoustic marks were identified and manually bounded by 'region' polygons (interpretation masks) which were labelled by mark type. Consistent with previous surveys, in 2022 SBW marks were identified and attributed to adults (spawning fish), immature fish (mainly 2 year olds), and juvenile fish (1 year old). Although the classification of marks was subjective, it followed the multiple lines of evidence approach which included information on mark appearance (e.g., shape, structure, strength, and compactness), the context (e.g., time of day/night, depth of the mark, bottom mark, and area), behaviour, mark identification trawls, expert knowledge as well as descriptions available studies of SBW mark classification and reports from previous surveys (e.g., Hanchet et al. 2002, O'Driscoll et al. 2018).

Acoustic backscatter data within regions labelled as adult, immature, and juvenile SBW were then echo-integrated to produce acoustic density estimates (in $km^2\ m^{-2}$). A constant sound absorption of 9.40 dB km^{-1} and a constant sound velocity of 1483 m s^{-1}, based on CTD data collected during the 2022 acoustic survey, were used for echo-integration (Appendix 2).

Total acoustic backscatter used for biomass estimation (Section 2.7) was extracted by taking the average of the acoustic backscatter from each transect. Density maps were also obtained by slicing the transects into 10-ping bins, giving a resolution of about 100 m at survey speed of 10 knots (see Section 3.4).

2.7 Biomass estimation

Acoustic density estimates from each stratum were converted to SBW biomass using the ratio, r, of mean weight to mean backscattering cross-section (linear equivalent of target strength).

Backscattering cross-sections were calculated from the scaled length frequency distribution (fork lengths) for three fish categories: juvenile, immature, and adult SBW, using the most recent target-strength-to-fork-length (TS-FL) relationship for SBW of O’Driscoll et al. (2013):

$$TS = 22.06 \log10 FL - 68.54 \qquad (2)$$

where TS is in dB re 1 m^2 and FL in cm.

The scaled length frequency distribution for adult SBW was estimated from the scientific observer data. Length frequency data from the mark identification trawling during the 2022 survey were used to estimate the scaled length frequency for juvenile SBW. Because no mark identification was carried out on immature marks of SBW in 2022, we used length frequency data from the 2019 Campbell Island acoustic survey (Ladroit et al. 2020b) to estimate the scaled length frequency for immature SBW.

Fish weights were calculated using the length-weight relationship for spawning SBW from Hanchet (1991):

$$w = 0.00439\ FL^{3.133} \qquad (3)$$

where weight (w) is in grams and FL is the fork lengths from the scaled length frequency distribution for each fish category.

Mean backscattering cross-section and mean weight for each fish category were obtained by calculating the mean of the transformed distribution obtained by equations 2 and 3, respectively.

Biomass estimates and their variances were obtained for each snapshot for juvenile, immature, and adult SBW using the formulae of Jolly & Hampton (1990). For each stratum, mean density of SBW for each fish category was multiplied by the stratum area to obtain the biomass; these values were then summed over all strata to produce an estimate for the snapshot. The values for the two snapshots were then averaged to produce a biomass estimate for the survey. The sampling precision (CV) of the mean biomass estimate from the survey combined the variance from each snapshot, using the assumption that each snapshot was independent.

Consistent with previous estimates, no transducer motion correction (Dunford 2005) was applied to biomass estimates, because measurements of towed body pitch and roll are not available for all surveys in the time series. O'Driscoll et al. (2007) indicated that compensating for motion correction increased biomass by only 3–10% in 2006. As expected, the magnitude of the change due to motion correction was related to mark depth (i.e., larger effect with increasing depth) and sea conditions (i.e., larger effect in poor conditions when there was greater motion).

3. RESULTS

3.1 Data collection

The weather conditions encountered during the survey period were challenging with a series of fronts passing through the survey area (Figure 6). We had to seek shelter near Campbell Island twice during the survey, on 3–6 and 12–14 September, with winds gusting up to 73 knots and swells up to 10 m. We estimated that about 190 hours (around 8 days) of survey time were lost due to weather. Due to the time lost, and taking into account the fish distribution, the survey area was modified to make the best possible use of the survey time available to achieve the specific objectives of this project.

All acoustic transects in the 2022 acoustic survey of the Campbell Island Rise stock of SBW were carried out using the DuFT. The use of the DuFT allowed the collection of acoustic data of good quality during the survey despite the adverse weather conditions faced. The average wind speed during the survey was 29 knots (standard deviation 8.6 knots) which was higher than the accepted limit for carrying out acoustic surveys using hull-mounted acoustic systems (25 knots).

Snapshot 1 took place between 30 August and 12 September 2022. Snapshot 1 started in stratum 11 at the northern area of the Campbell Island Rise, progressed east and then southeast covering the eastern strata (5–8), and finished in stratum 7S south of Campbell Island (see Figure 4). Due to time constrains and location of fish, three planned transects were not completed (one in stratum 6S and two in stratum 7S). Snapshot 1 consisted of 52 acoustic transects and 5 mark identification bottom trawls. A summary of the transects and mark identification trawls completed in snapshot 1 is available in Table 1.

Snapshot 2 was carried out between 12 and 20 September 2022. As noted in Section 2.1, information on the distribution of SBW during snapshot 1 and the location of the fishing fleet were used to modify the survey boundaries for snapshot 2. Snapshot 2 started in stratum 7S and continued northeast until 13 September when due to bad weather the survey was paused. The survey was resumed on 16 September 2022 north of Campbell Island in stratum 11. From there, the survey continued east covering strata 2–4, and then south and east surveying strata 5–8. The detection of spawning aggregation of SBW at the eastern boundary of stratum 8 (see Figure 5), required the addition of a new stratum (stratum 12), where an aggregation-based snapshot was completed. Thus, snapshot 2 consisted of 10 strata and 41 acoustic transects (see Table 4). Seven mark identification trawls were carried out during snapshot 2; three bottom and four midwater trawls.

A total of 2.5 TB of acoustic data were collected using RV *Tangaroa'*s hull echosounder system and 90 GB using the DuFT. These data were stored in the NIWA *acoustics* database.

3.2 Mark identification trawling

Mark identification trawling in the 2022 SBW acoustic survey was restricted due to time constraints, and only 12 trawls were carried out (Table 4). During the first snapshot most trawls were carried out in the northern strata (i.e., 11, 2–4). The mark types targeted were associated with juvenile SBW, which were found shallower than 400 m (Figure 7), and deep hazy marks (bottom depth > 500 m) which contained low proportions of adult SBW.

A dense midwater pre-spawning aggregation of SBW was detected after dusk in the northern area (stratum 2) during snapshot 1 (Figure 8). Because the commercial fleet was operating in the vicinity (see Section 3.3), no research mark identification trawl was carried out on this mark. Adult marks of pre- and spawning SBW have been well documented (e.g., Hanchet et al. 2002, O'Driscoll et al. 2018, Ladroit et al. 2020b), hence their identification on echograms is straightforward.

A second midwater aggregation of adult SBW was detected in stratum 7S during the first snapshot (Figure 9). Due to an approaching weather front, this aggregation was targeted approximately 24 hours later during the start of snapshot 2 to prioritise the completion of the acoustic transects of snapshot 1. The aggregation was observed in both snapshots at similar depths (centred around 300 m depth) and two midwater trawls were carried out on it at night. The catches were dominated in weight and number by pre-spawning adult SBW (Table 4).

A third midwater aggregation of SBW was found east of Campbell Island, at the eastern boundary of the stratum 8 of snapshot 2 (see Figure 5). Upon the completion of an aggregation-based snapshot (stratum 12), one midwater trawl was carried out on the SBW mark. The aggregation consisted almost exclusively of adult SBW (Table 4), some of which were actively spawning (about 40% of female fish were spawning – stage 4 and 5, see Appendix 3).

During snapshot two, further mark identification trawls (n = 3) were carried out on marks of juvenile SBW, where the composition of SBW varied from 22 to 96% (Table 4). No mark identification trawling was carried out on immature SBW marks (Figure 10) in the 2022 acoustic survey.

Because of the small number of trawls and uncertainty associated with the relative catchabilities of different species, no species decomposition of acoustic backscatter was attempted for the analysis. All backscatter from adult, immature, and juvenile SBW marks was assumed to be from SBW consistent with previous years and supported by most previous trawl catches (Hanchet et al. 2003, O'Driscoll et al. 2007, Gauthier et al. 2011, O’Driscoll 2011, O’Driscoll et al. 2012, O’Driscoll et al. 2014, O’Driscoll et al. 2018, Ladroit et al. 2020b).

3.3 Commercial data

A total of 503 target SBW tows were reported by electronic catch reporting (ERS) from the Campbell Island grounds between 22 August and 24 September 2022. The total estimated catch for this period was of 21 300 t of SBW. This was slightly lower than the reported (Monthly Harvest Return) catch of 22 983 t for SBW 6I, and below the TACC of 39 200 t. Fishing effort was concentrated mainly in the northern area with 15 114 t of SBW catch. Fishing effort was also observed in the southern and eastern areas, with 4357 t of SBW catch from the south and 1829 t from the east. During snapshot 1 fishing effort was confined to strata 11, 2, and 4 (Figure 11). During snapshot 2, the effort was distributed between the northern (mostly stratum 2 but also in stratum 4) and southern strata (7S) (Figure 11). Fishing in the eastern strata was conducted after snapshot 2 mainly in stratum 8 (effort not shown here).

Two distinct spawning periods (defined as when the proportion of running ripe females exceeded 10%) were recorded, during 23–29 August and 11–22 September (Figure 12). The timing of the first spawning in 2022 was early compared with the timing in previous years. The timing of the second spawning event was similar to 2016 and early compared with the timing in 2019.

The scaled length frequency distributions of SBW caught by commercial vessels are shown in Figure 8. Of the 503 commercial trawls, 367 trawls were carried out in the northern strata (strata 11, 2, 3N, 3S, 4, and 5) with 17 392 SBW measured. In the southern area 80 trawls were carried out within the boundaries of stratum 7S and 11 trawls were carried out outside the strata definitions (east of stratum 7S) during snapshot 2, with a total of 3048 SBW measured. In the eastern strata (i.e., 6N, 6S, 8N, 8S, and 8E in snapshot 1, and 6, 8 and 12 in snapshot 2), 45 trawls were carried out, with 1993 SBW measured. Length distributions were unimodal for both males and females in the north, with the mode for males centred on 37 cm and the mode for females centred on 39 cm (Figure 13). Length distributions were unimodal for males and bimodal for females in the south, with the mode for males centred on 37 cm and the modes for females centred around 40 and 48 cm. The length distributions in the east were unimodal for males, centred around 41 cm, and bimodal for females with a main mode centred at 50 cm and a secondary mode centred around 39 cm (Figure 13). The mean length for adult SBW in the east was 44.6 cm, which was much higher than that in the north and south at 39.3 and 39.9 cm, respectively (Table 5).

3.4 Spatial distribution of backscatter

Spatial distribution of acoustic backscatter for both snapshots are shown in Figure 14 for adult SBW marks, in Figure 15 for immature SBW marks, and Figure 16 for juvenile SBW. During snapshot 1 aggregations of adult SBW were detected in strata 2 and 4, with the main aggregation at the eastern boundary of stratum 2. For the second snapshot, the spatial distribution of backscatter associated with adult SBW was more spread across the northern strata. The spatial distribution of backscatter of adult SBW during snapshot 1 was relatively consistent with the distribution of commercial catch, except for in stratum 11, where the commercial catches took place after the stratum was surveyed acoustically (see Figure 11). During snapshot 2 the spatial distribution of backscatter associated with adult SBW and commercial catches only overlapped in stratum 2, as the bulk of the fishing effort had moved to the southern area (see below).

The spatial distribution of acoustic backscatter associated with adult SBW in the southern area was concentrated in stratum 7S in both snapshots (both were completed within 48 hours). The spatial distribution of the commercial catches and backscatter of adult in the southern area were very consistent (see Figures 14 and 11). Marks of adult SBW were found in the eastern area during snapshot 2 (mainly stratum 12). Commercial catches of adult SBW were made in this area after the completion of snapshot 2.

The spatial distribution of backscatter associated with immature SBW marks was consistent along the southern end of strata 2 and 4 and western end of stratum 5 (Figure 15), typically at bottom depths shallower than 410 m (but slightly deeper to the west of Campbell Island). This spatial distribution was consistent between snapshots.

The spatial distribution of backscatter associated with juvenile SBW marks was very extensive and consistent at the shallower end (typically shallower than 350 m but also down to a maximum depth of 400 m) of strata 2, 4, 5, and 7N in snapshot 1, and of strata 11, 2, 4, 5, 7N, and 7S in snapshot 2 (Figure 16).

3.5 Size and maturity

Length, sex, and stage were determined from 1158 SBW sampled during the acoustic survey in 2022 (Table 6). The scaled length frequency distributions from research mark identification trawls on adult and juvenile SBW marks are compared in Figure 13 and summarised in Table 5. Overall, the modes from the length frequency distributions from research trawls were 1–3 cm smaller than those of the length frequency distributions from commercial data (Figure 13).

The average size of adult SBW estimated from three mark identification trawls in the northern area (mean length 38.3 cm) were larger than that from two mark identification trawls in the southern area (mean length 36.8 cm). Despite the low number of mark identification trawls, this difference might reflect a gear selectivity effect (i.e., trawls in the northern area were bottom trawls carried out using the ratcatcher with a 40 mm codend, while those in the southern area were carried out with the fine-mesh midwater trawl with 10 mm codend), differences in vertical distribution and/or behaviour of adult SBW (i.e., trawls in the northern area were carried out during the day on the bottom and in the southern area were carried out at night in midwater), and/or differences in size structure (i.e., fish belonging to different sub-stocks). However, the average length from commercial data, thought to be more representative of the size of fish in the spawning aggregations, showed very similar average lengths for the northern and southern areas (39.3 cm in the north versus 39.9 cm in the south, see Table 5), so it is unlikely that the northern and southern fish had different size structure in 2022.

The average size of adult SBW from the eastern area from one mark identification trawl (mean length 44.5 cm) was much larger than that from the northern and southern areas. This was very consistent with the average length from commercial data based on 45 trawls (mean length 44.6 cm).

Juvenile SBW caught from immature SBW marks had a single mode between 18 and 20 cm and were probably 1 year old (2021 year class).

Since the main objective of research mark identification trawls is not to sample the main spawning aggregations where the commercial fleet operates (see Section 2.3) and the sampling was very restricted due to time availability, the timing of spawning cannot be inferred from the research data. Almost all adult female SBW caught in snapshots 1 and 2 in northern and southern areas were pre-spawning (stage 3) (Table 6). Female SBW sampled in the eastern area were either ripening (34 %), running ripe (38%), or partially spent (17%). Juvenile SBW were almost exclusively at stage 1 (males and females).

3.6 Biomass estimates

Biomass estimates for SBW were calculated from acoustic density estimates using the weight-to-backscattering ratio *r* values in Table 5, which were computed using length frequency distributions shown in Figure 13. Because the length frequency data from the commercial data are considered to be more representative of the size of fish in the spawning aggregations (e.g., much larger sampling effort well distributed over areas where aggregations of adult SBW were observed), data from the commercial fishery were used to estimate the ratio *r* in the northern, southern, and eastern areas. Length frequency data from mark identification trawls from the 2022 acoustic survey were used to estimate the ratio *r* for juvenile SBW marks, and from the 2019 acoustic survey to estimate the ratio *r* for immature SBW.

Biomass estimates for juvenile, immature, and adult SBW are given by snapshot and stratum in Table 7 and by sub-areas in Table 8. The total adult biomass estimate was 87 919 t (CV 26%) in snapshot 1 and 96 016 t (CV 23%) in snapshot 2. At the Deepwater Working Group meeting on 10 November 2022, it was agreed to use the average of the two snapshots as the biomass index for 2022. The average was 91 986 t (CV 20%), which was very similar to the estimate from the last survey in 2019 (91 145 t, CV 27%) (Table 9).

The estimates of biomass in snapshot 1 were highest in the northern (strata 2 and 4) and southern (stratum 7S) areas, which coincided with the areas where large aggregations of adult SBW were observed. This was relatively consistent with the estimates in snapshot 2; however, in snapshot 2 the biomass was more spread across strata in the north (Table 7). Biomass was highest in snapshot 2 in stratum 7S (Table 7).

Although no spawning aggregation was detected during snapshot 1 on the eastern area (strata 6N, 6S, 8N, 8S, and 8E), the biomass estimates between snapshots for the area were similar (Table 8). Although a spawning aggregation was observed in snapshot 2 in the eastern area (stratum 12), its overall contribution to the area was modest due to the small size of the stratum.

The biomass estimates between snapshots in 2022 were more consistent than those obtained in 2019 when the biomass between snapshots in the eastern and southern areas almost halved between snapshots 1 and 2. Compared with the overall biomass estimates for adults from the 2019 acoustic survey, the overall biomass in 2022 was over two times higher in the northern area, similar in the eastern area (with a lower CV), and about 50% lower in the southern area.

The estimates of biomass for immature SBW biomass were 6933 t (CV 21%) in snapshot 1 and 3779 t (CV 49%) in snapshot 2, averaging to 5356 t (CV 22%) (Table 9). This estimate was about 27% higher than that from 2019.

The estimates of biomass for juvenile SBW biomass were 11 549 t (CV 17%) in snapshot 1 and 13 980 t (CV 22%) in snapshot 2, averaging to 12 764 t (CV 14%) (Table 9). The estimates from the 2022 acoustic survey were the highest of the time series for juvenile SBW.

4. DISCUSSION

The 2022 acoustic survey of the Campbell Island stock of SBW was carried out between 28 August and 23 September 2022 onboard RV *Tangaroa*. Two acoustic snapshots, both carried out with the DuFT, and twelve research mark identification trawls were completed. Aggregations of adult SBW were observed in the northern and southern areas of the survey during snapshot 1 and in the northern, southern, and eastern areas during snapshot 2. While commercial length frequency data from the Campbell Island Rise spawning fishery were used to convert acoustic densities associated with adult SBW to biomass, length frequency data from research mark identification trawls from 2022 and 2019 were used to estimate the biomass of juvenile and immature SBW, respectively. The average biomass of adult SBW for 2022 was 91 968 t (20% CV), which was very similar to the previous estimate from 2019.

4.1 Timing of the survey

The timing and duration of the survey was similar to the previous eight surveys between 2002 and 2019 (Figure 12). Data from scientific observers in SBW6I indicate that there were two spawning events in 2022. Compared with previous years, the first spawning event in 2022 occurred between 23 and 30 August, the earliest recorded in the time series (see Figure 12). The timing of the second spawning event (12–23 September) was similar to that of the first spawning events observed in 2009 and 2011 (Figure 12). Although the timing of the spawning in 2022 was early, and the timing of the first acoustic snapshot (30 August–11 September) did not cover the first spawning event and rather surveyed the pre-spawning period of the second event, the biomass estimates obtained from both snapshots were consistent (see Table 7). Once SBW move into the spawning grounds (i.e., survey area) they are thought to remain in the area between spawning events and be available to be surveyed using acoustics. Consequently, and because the timing of the second snapshot was conducted during the second spawning event between 12 and 20 September, we believe the timing of the 2022 survey was suitable as adult SBW were available in the survey area during both snapshots.

4.2 Spatial coverage of survey

Three main aggregations of adult SBW were found in the northern and southern areas in snapshot 1 and in the northern, southern, and eastern areas in snapshot 2. Historically, fishing effort in SBW 6I has concentrated in the northern (or northeastern) and southern areas. Since 2002, there has been increasing commercial fishing effort outside the historical core survey area (strata 2 to 7, e.g., Figure 2), with commercial catches reported in 2021 west of stratum 2 outside the core survey area, which led to the addition on a new stratum 11 for the 2022 survey (see Figure 3). Although no adult SBW was detected in this stratum during snapshot 1, it was retained for snapshot 2 because of the observed distribution of fishing effort during the survey. The biomass contribution from stratum 11 compared with other strata was relatively low; however, stratum 11 still accounted for about 5% of the total estimate of snapshot 2.

Prior to the 2011 survey, only a single aggregation was observed in the northeast of the survey area. In 2011 and 2013 two distinct aggregations were observed in the north and in the east (O'Driscoll et al. 2012, O'Driscoll et al. 2014). The spatial distribution of commercial catch in 2011, 2012, 2015, 2017, and 2019, and the acoustic surveys in 2016 and 2019, also support an eastern aggregation (note that the encounter of adult aggregations of SBW by the research vessel in survey years away from the commercial fleet can influence the distribution of SBW catch rates in SBW 6I). In 2022, an eastern aggregation was also detected during snapshot 2 and surveyed using an aggregation-based snapshot (stratum 12). Although the contribution of stratum 12 in terms of biomass to the overall estimate was not substantial due to its small area (see Table 2), the eastern area accounted for 19% of the estimated biomass of adult SBW on the Campbell Island Rise.

The spatial distribution of biomass of adult SBW on the Campbell Island Rise varies considerably between surveys. Very dense spawning marks have been detected in the southern area of the survey, resulting in the southern aggregation accounting for up to 52% of the estimated adult acoustic biomass on the Campbell Island Rise between 2009 and 2022 (peak recorded in 2019, see Table 10). In 2013, despite extensive searching, no spawning SBW were detected in the southern area (O'Driscoll et al. 2014). Low catch rates in the southern area confirmed the decline of adult SBW observed in the survey in 2013; however, the spawning aggregation seems to have progressively reappeared in the south with increasing commercial catches between 2014 and 2016 (O'Driscoll et al. 2018) and made an important contribution to the total biomass estimates of adult SBW in 2019 and 2022.

Although the northern area has been the most consistent over the time series of acoustic estimates of biomass (i.e., spawning aggregations have been always found in this area), its contribution also fluctuates substantially between surveys. In the 2022 survey, the northern area accounted for 50% of the biomass which was above the average (41%) for the time series since 2011, when the eastern area was first identified as holding a distinct spawning aggregation (O'Driscoll et al. 2012). The contribution of the eastern area in 2022 to the average biomass estimate (19%) was similar to that in 2019 (Table 10).

Considering the temporal and spatial variability in the indices of abundance and the changes in the spatial distribution of SBW and fishing effort, we recommend that the survey area and stratification continue to be reviewed before future surveys.

4.3 Size structure between survey areas

Length frequency data from mark identification trawls and scientific observers showed that adult SBW from the northern and southern areas had very similar size distributions (mean length from observer data 39.3 and 39.9 cm, respectively), which were different from adult SBW from the eastern area where larger fish were found (observer data mean length of 44.6 cm).

The size structure of adult SBW on the Campbell Island Rise has varied over time, but typically there is similar size structure between aggregations. Hanchet (2005) examined commercial length frequency data from 1997 to 2004 and found that SBW caught east of the core area had a similar size distribution to those caught in the north within the core area; he concluded that changes in fish spatial distribution were likely due to fish movement rather than the existence of an unrecorded population.

The current accepted stock structure for the Campbell Island Rise assumes a single stock, which can be distinguished from other stocks (e.g., SBW 6B) on the basis of their morphometric measurements (Large et al. 2021). Comparisons of length-to-weight relationships of adult SBW from the 2022 scientific observer data showed that the different areas of SBW 6I conform to the length-weight relationship from Hanchet (1991), further supporting the hypothesis of a single stock of the Campbell Island Rise.

The average lengths for the three areas were the highest recorded over the last 15 years, reflecting growth of older fish and lack of recent recruitment. The incidence of fish over 35 cm in 2019 (Ladroit et al. 2020b) was linked to the 2009 and 2011 year classes which were estimated as being relatively strong (Large et al. 2021). Fish from these year classes are still present in the fishery and are responsible for the larger average lengths observed in 2022. The 2014 and 2015 year classes have also been regarded as relatively strong (Large et al. 2021). Conversely, below average estimates of biomass of immature SBW in 2019 and analysis of commercial catch proportions-at-age suggested that the 2016 and 2017 year classes were not strong.

Immature (25–35 cm) SBW probably reflect the 2019 and 2020 year classes (2–3 year olds) and juveniles (15–25 cm) are likely the 2021 year class (1 year old).

4.4 Variability between snapshots

The two snapshot estimates of biomass of adult SBW from the 2022 acoustic survey were very consistent, with the estimate from snapshot 2 being 9% higher than that from snapshot 1. The spatial distribution was also consistent between snapshots (see Table 8). The estimates of biomass of adult SBW between snapshots in 2022 were the second most consistent in the time series, after the estimates from 2000 when the difference between snapshots was only 5% (Hanchet & Grimes 2001).

The similarity between snapshot estimates contrasts markedly with 2019, when the difference between snapshots was close to 50% (Ladroit et al. 2020b), and with 2016 when there was a four-fold difference between snapshots 1 and 2 (Figure 17). The 2016 survey was also the only one where the two snapshot estimates did not have overlapping 95% confidence intervals (Figure 18). This was because only weak adult marks were detected in the east in snapshot 1, whereas extensive post-spawning marks were detected a week later in snapshot 2 (O'Driscoll et al. 2018). O'Driscoll et al. (2018) explored various hypotheses to explain the low estimated biomass of adult SBW in the eastern area during snapshot 1 in

2016 and noted that it was not statistically appropriate to average abundance estimates from this region from the two snapshots.

The estimate of biomass for juvenile SBW was about 20% higher in snapshot 2 but was still statistically comparable with the estimate of snapshot 1. Estimates of juvenile SBW are expected to be highly variable because the stratum definitions of the survey do not encompass the whole distribution range of juvenile SBW. Juvenile SBW are believed to be pelagic and information from tracking studies of albatrosses suggests that they found in much shallower water than the shallower end of the survey area (200 m) (Cherel et al. 1999).

The biomass of immature SBW almost halved between snapshot 1 and snapshot 2. Biomass of immature SBW has been highly variable between snapshots (about 80% lower in snapshot 2 compared with that in snapshot 1 in 2016), except in 2019 when it was very similar (about 2% difference). Differences in the biomass of immature SBW between snapshots might be related to fish movement or mixing with juvenile or adult marks. Increasing the number of mark identification trawls (typically limited due to time constraints) could provide additional information regarding the variability of immature SBW between snapshots.

4.5 Comparison between years

The estimated biomass of adult SBW was 91 968 t in 2022 and was above the average for time series. The estimate was similar to that from the two most recent acoustic surveys in 2016 (O'Driscoll et al. 2018) and 2019 (Ladroit et al. 2020b) (see Table 9). This apparent recent stability of adult biomass of SBW could be related to the above-average recruitment of the 2009, 2011, 2014, and 2015 year classes into the fishery and the sustained moderate commercial catches of SBW around the Campbell Island Rise over the last seven fishing years compared with historical catch levels (the average landings between the fishing years 2016–17 and 2022–23 was 18 561 t compared with 23 836 t between the 2009–10 and 2015–16 fishing years) (Fisheries New Zealand 2022).

The estimated biomass of immature SBW was 5356 t in 2022 and was below average for the time series but higher than in 2016 and 2019. This suggests that the 2019 and 2020 year classes (ages three and two, respectively) were not abundant. This was consistent with the previous estimates of immature SBW that since 2009, when the biomass of immature SBW was the second highest of the time series (strong year classes 2006 and 2007), have remained relatively low (see Table 9).

The estimated biomass of juvenile SBW was 12 762 t in 2022 and was the highest in the time series of acoustic surveys of the Campbell Island Rise. The high estimate was expected due the observation of extensive dense aggregations associated with juvenile SBW across most of the strata in both snapshots. These findings suggest that the 2021 year class was strong. However, since little is known about the distribution of juvenile SBW around Campbell Island, it is not possible to compare changes in abundance or availability in the survey grounds with previous years.

5. ACKNOWLEDGEMENTS

Thanks to Evan Solly (skipper) and the crew of RV *Tangaroa* who were responsible for the success of the 2022 acoustic survey of SBW on the Campbell Island Rise (TAN2210). Also thanks to the voyage participants: Alicia Maurice, Alina Wieczorek, Chris Ray, Steven George, and Darren Stevens. Finally, thanks to Dan MacGibbon, Mark Fenwick, Jason Hamill, and Brian Parata for preparing, mobilising, and demobilising the gear required for the survey. Special thanks to Richard O'Driscoll for his help with the acoustic data analysis and valuable comments and discussions around the annotation of echograms and biomass indices of SBW. This work was funded under Fisheries New Zealand project SBW2021-01. This report was reviewed by Darren Stevens.

6. REFERENCES

Cherel, Y.; Waugh, S.; Hanchet, S. (1999). Albatross predation of juvenile southern blue whiting (*Micromesistius australis*) on the Campbell Plateau. *New Zealand Journal of Marine and Freshwater Research 33*: 437–441.

Demer, D.A.; Berger, L.; Bernasconi, M.; Bethke, E.; Boswell, K.; Chu, D.; Domokos, R.; et al. (2015). Calibration of acoustic instruments. *ICES Cooperative Research Report No. 326*. 133 p.

Doonan, I.J. (2020). Southern blue whiting (*Micromesistius australis*) stock assessment for the Campbell Island Rise for data up to 2018–19. *New Zealand Fisheries Assessment Report 2020/43*. 20 p.

Dunford, A.J. (2005). Correcting echo-integration data for transducer motion. *The Journal of the Acoustical Society of America 118*: 2121–2123.

Dunn, A.; Grimes, P.J.; Hanchet, S.M. (2001). Comparative evaluation of two-phase and adaptive cluster sampling designs for acoustic surveys of southern blue whiting (*Micromesistius australis*) on the Campbell Rise. (Final Research Report for Ministry of Fisheries Research Project SBW1999/01 Objective 1. National Institute of Water and Atmospheric Research. 15 p.)

Dunn, A.; Hanchet, S.M. (1998). Two-phase acoustic survey designs for southern blue whiting on the Bounty Platform and the Pukaki Rise. *NIWA Technical Report 28*. 29 p.

Fisheries New Zealand (2021). Review of Sustainability Measures for Southern Blue Whiting (SBW 6B) for 2022/23. *Fisheries New Zealand Discussion Paper No: 2021/28*. 16 p.

Fisheries New Zealand (2022). *Fisheries Assessment Plenary, May 2022: stock assessments and stock status*. Compiled by the Fisheries Science Team, Fisheries New Zealand, Wellington, New Zealand. 1886 p.

Fofonoff, P.; Millard, R., Jr. (1983). Algorithms for computation of fundamental properties of seawater. *UNESCO Technical Papers in Marine Science 44*: 53–53.

Fu, D.; Hanchet, S.; O'Driscoll, R. L. (2013). Estimates of biomass and c.v.s of southern blue whiting from previous acoustic surveys from 1993 to 2012 using a new target strength – fish length relationship. Final Research Report for Ministry for Primary Industries Research Project DEE201002SBWB. 52 p. (Unpublished report held by Fisheries New Zealand, Wellington.)

Gauthier, S.; Fu, D.; O'Driscoll, R.L.; Dunford, A. (2011). Acoustic estimates of southern blue whiting from the Campbell Island Rise, August–September 2009. *New Zealand Fisheries Assessment Report 2011/9*.

Grimes, P.J.; Hanchet, S.M. (1999). Acoustic biomass estimates of southern blue whiting (*Micromesistius australis*) from the Bounty Platform and Pukaki Rise, August-September 1997. New Zealand Fisheries Assessment Research Document 99/12. 28 p. (Unpublished report held by NIWA library, Wellington.)

Hanchet, S. M. (1991). Southern blue whiting fishery assessment for the 1991–92 fishing year. New Zealand Fisheries Assessment Research Document 91/7. 48 p. (Unpublished report held by NIWA library, Wellington.)

Hanchet, S. M. (1993). Southern blue whiting (*Micromesistius australis*) fishery assessment for the 1993–94 fishing year. New Zealand Fisheries Assessment Research Document 93/17. 56 p. (Unpublished report held by NIWA library, Wellington.)

Hanchet, S.M. (2005). Southern blue whiting (*Micromesistius australis*) stock assessment update for the Campbell Island Rise for 2005. *New Zealand Fisheries Assessment Report 2005/40*. 40 p.

Hanchet, S.M.; Grimes, P.J. (2001). Acoustic biomass estimates of southern blue whiting (*Micromesistius australis*) from the Campbell Island Rise and Pukaki Rise, September 2000. *New Zealand Fisheries Assessment Report 2001/58*. 37 p.

Hanchet, S.M.; Grimes, P.J.; Coombs, R.F.; Dunford, A. (2003). Acoustic biomass estimates of southern blue whiting (*Micromesistius australis*) for the Campbell Island Rise, August-September 2002. *New Zealand Fisheries Assessment Report 2003/44*. 38 p.

Hanchet, S.M.; Grimes, P.J.; Dunford, A.; Ricnik, A. (2002). Classification of fish marks from southern blue whiting acoustic surveys. Final Research Report for Ministry of Fisheries Research Project SBW2000/02 Objective 2. 55 p. (Unpublished report held by Fisheries New Zealand, Wellington.)

Hanchet, S. M.; Haist, V. (1994). Southern blue whiting (*Micromesistius australis*) fishery assessment for the 1994–95 fishing year. New Zealand Fisheries Assessment Research Document 94/22. 41 p. (Unpublished report held by NIWA library.)

Jolly, G.M.; Hampton, I. (1990). A Stratified Random Transect Design for Acoustic Surveys of Fish Stocks. *Canadian Journal of Fisheries and Aquatic Sciences 47 (7)* : 1282–1291.

Ladroit, Y.; Escobar-Flores, P. C.; Schimel, A. C. G.; O'Driscoll, R. L. (2020a). ESP3: An open-source software for the quantitative processing of hydro-acoustic data. *SoftwareX 12*: 100581–100581.

Ladroit, Y.; O'Driscoll, R. L.; Large, K. (2020b). Acoustic estimates of southern blue whiting from the Campbell Island Rise, August-September 2019 (TAN1905). *New Zealand Fisheries Assessment Report 2020/26*. 60 p.

Large, K.; O'Driscoll, R. L.; Datta, S. (2021). Review and summary of the time series of input data available for the assessment of southern blue whiting (*Micromesistius australis*) stocks up to and including the 2020 season. *New Zealand Fisheries Assessment Report 2021/40*. 73 p.

McClatchie, S.; Thorne, R.; Grimes, P. J.; Hanchet, S. (2000). Ground truth and target identification for fisheries acoustics. *Fisheries Research 47*: 173–191.

O'Driscoll, R.L. (2011). Acoustic biomass estimates of southern blue whiting on the Pukaki Rise and Campbell Island Rise in 2010. NIWA Client Report WLG2011-03 for The Deepwater Group Ltd. 37 p. (Unpublished report available from Deepwater Group Ltd, Auckland.)

O'Driscoll, R.L.; Dunford, A.J.; Fu, D. (2012). Acoustic estimates of southern blue whiting from the Campbell Island Rise, August–September 2011 (TAN1112). *New Zealand Fisheries Assessment Report 2012/18*. 56 p.

O'Driscoll, R.L.; Dunford, A.J.; Ladroit, Y. (2014). Acoustic estimates of southern blue whiting from the Campbell Island Rise, August–September 2013 (TAN1309). *New Zealand Fisheries Assessment Report 2014/22*. 50 p.

O'Driscoll, R.L.; Hanchet, S.M. (2004). Acoustic survey of spawning southern blue whiting on the Campbell Island Rise from FV Aoraki in September 2003. *New Zealand Fisheries Assessment Report 2004/27*. 31 p.

O'Driscoll, R.L.; Hanchet, S.M.; Gauthier, S.; Grimes, P.J. (2007). Acoustic estimates of southern blue whiting from the Campbell Island Rise, August-September 2006. *New Zealand Fisheries Assessment Report 2007/20*. 34 p.

O'Driscoll, R.L.; Large, K.; Marriott, P. (2018). Acoustic estimates of southern blue whiting from the Campbell Island Rise, August–September 2016 (TAN1610). *New Zealand Fisheries Assessment Report 2018/56*. 60 p.

O'Driscoll, R.L.; Macaulay, G.J.; Gauthier, S. (2006). Biomass estimation of spawning southern blue whiting from industry vessels in 2006. NIWA Client Report: WLG2006-89 for the Deepwater Stakeholders Group Ltd. 43 p. (Unpublished report available from Deepwater Group Ltd, Nelson.)

O'Driscoll, R.L.; Oeffner, J.; Dunford, A.J. (2013). In situ target strength estimates of optically verified southern blue whiting (*Micromesistius australis*). *ICES Journal of Marine Science* 70: 431–439.

7. TABLES

Table 1: Summary of transects and trawls carried out during snapshot 1 of the 2022 SBW acoustic survey of the Campbell Island Rise. Transect positions are plotted in Figure 4. Planned snapshot 1 transect allocation was based on historical catch rates and commercial tow positions. Strata 2–7 are core strata which have been surveyed in all previous acoustic surveys. During the survey stratum 7S was extended to 169° 10’ E to the west and to 53° 06’ S to the south, while its eastern boundary was shortened to 170° 20’ E; the southern boundary of stratum 6S was shortened to 53° 12’ S. Revised areas in the table are shown in bold and original areas are provided in parentheses.

		Number of transects		Number of
Stratum	Area (km^2)	Planned	Completed	trawls
2	3 154	5	5	1
3N	2 342	3	3	
3S	1 013	3	3	1
4	2 690	5	5	1
5	3 029	4	4	1
6N	1 150	4	4	
6S	**2 505** (3 025)	3	2	
7N	2 980	4	4	
7S	**3 028** (3 815)	8	6	
8N	1 436	3	3	
8S	1 452	3	3	
8E	4 648	6	6	
11	2 196	4	4	1
Total	31 623 (32 930)	55	52	5

Table 2: Summary of transects and trawls carried out during snapshot 2 of the 2022 SBW acoustic survey of the Campbell Island Rise. Transect positions are plotted in Figure 5. Planned snapshot 2 transect allocation was based on mean fish densities observed in snapshot 1 and commercial tow positions. Strata 3S and 3N were not surveyed in snapshot 2. Strata 6N and 6S were combined into a smaller stratum 6, which had a new southern boundary at 52° 40’ S. Strata 8N, 8S, and 8E were combined into a single stratum 8, which was reduced on its eastern boundary to 171° 50’ E. Stratum 7S was shortened at its southern boundary to 53° 30’ S. Stratum 12 was an aggregation-based snapshot.

Stratum	Area (km^2)	Number of transects Completed	Number of trawls
2	3 154	4	2
3S	1 013	3	
4	2 690	4	
5	3 029	4	2
6	2 324	4	
7N	2 980	3	
7S	2 367	7	2
8	5 230	4	
11	2 196	3	
12	67	5	1
Total	25 050	41	7

Table 3: Echosounder settings used for acoustic data collection on the dual frequency towed body (DuFT) and RV *Tangaroa* hull system during the 2022 acoustic survey of southern blue whiting of Campbell Island Rise. EK80 was the Simrad software used for data acquisition. WBT = wideband transceiver, GTP = general purpose transceiver.

DuFT		
Frequency (kHz)	38	120
Transceiver	WBT tube	WBT tube
EK80 software version	21.15.1	21.15.1
Transmit power (W)	1000	250
Pulse length (ms) CW/FM	1.024	1.024
Ping rate (ms)	1500	1500

Hull system					
Frequency (kHz)	18	38	70	120	200
Transceiver	WBT	GPT	WBTtube	GPT	GPT
EK80 software version	21.15.1	21.15.1	21.15.1	21.15.1	21.15.1
Transmit power (W)	1000	2000	750	250	150
Pulse length (ms) CW/FM	1.024/4.096	1.024	1.024/2.048	1.024	1.024
Ping rate (ms)	2000	2000	2000	2000	2000

Table 4: Station details and catch summary of southern blue whiting (SBW) from mark identification trawls completed during the 2022 acoustic survey of SBW of Campbell Island Rise. BT = bottom trawl, MW = midwater trawl.

										Catch weight (kg)		
Station	Snapshot	Stratum	Gear	Mark type	Date	Latitude	Longitude	Depth (m)	Distance (nm)	SBW	Total	% SBW
1	1	11	BT	Adult	1-Sep-22	51º23.40’	169º10.69’	535	1.50	8.6	141.8	6.1
2	1	2	BT	Juveniles	1-Sep-22	51º38.01’	169º17.61’	361	1.05	9.6	96.3	10.0
3	1	3S	BT	Adult	7-Sep-22	51º33.90’	170º39.98’	512	1.44	43.0	475.5	9.0
4	1	4	BT	Juveniles	7-Sep-22	51º48.14’	170º03.82’	357	3.67	1.0	2.1	47.6
5	1	5	BT	Juveniles	9-Sep-22	52º12.57’	170º19.40’	390	1.10	49.3	122.5	40.2
6	2	7S	MW	Adult	12-Sep-22	53º23.27’	169º29.84’	490	1.60	31.1	35.5	87.6
7	2	7S	MW	Adult	13-Sep-22	53º25.46’	169º29.56’	554	1.55	72.9	80.2	90.9
8	2	2	BT	Adult	17-Sep-22	51º37.17’	169º53.29’	420	1.09	129.7	184.5	70.3
9	2	2	BT	Juveniles	17-Sep-22	51º41.88’	169º52.80’	380	1.51	148.2	658.5	22.5
10	2	5	MW	Juveniles	18-Sep-22	52º07.53’	170º35.63’	399	2.16	28.4	29.6	95.9
11	2	5	BT	Juveniles	19-Sep-22	52º33.48’	170º06.50’	367	0.99	49.6	118.1	42.0
12	2	12	MW	Adult	19-Sep-22	52º18.95’	171º49.03’	443	2.46	225.7	229.0	98.6

Table 5: Estimates of the ratio *r* used to convert backscatter associated with southern blue whiting marks to biomass. Values are derived from the scaled length frequency distributions in Figure 13. Abundance estimates (Table 8) were calculated using *r* from commercial tows for adult SBW in the northern, southern, and eastern areas, and from research tows from the 2022 acoustic survey (TAN2210) for juvenile and from the 2019 acoustic survey (TAN1905) for immature SBW. σ is the acoustic backscattering coefficient, the linear equivalent of the target strength (TS).

Category	Data source	No. of trawls measured	Mean length (cm)	Mean weight (g)	Mean σ (m^2)	Mean TS (dB)	r (kg m^{-2})
Adult (north)	Commercial	367	39.3	443.3	0.000464	-33.33	955.0
Adult (south)	Commercial	91	39.9	475.7	0.000485	-33.14	981.0
Adult (east)	Commercial	45	44.6	676.2	0.000621	-32.07	1089.0
Adult (north)	Research – 2022	3	38.3	415.0	0.000442	-33.55	939.6
Adult (south)	Research – 2022	2	36.8	362.7	0.000403	-33.95	900.6
Adult (east)	Research – 2022	1	44.5	669.4	0.000617	-32.10	1084.4
Juvenile	Research – 2022	6	19.9	54.8	0.000105	-39.79	521.8
Immature	Research – 2019	6	29.2	173.0	0.000240	-36.20	721.0

Table 6: Gonad stages of southern blue whiting (SBW) sampled in mark identification trawls during the 2022 acoustic survey of the Campbell Island Rise (TAN2210). Gonad stages are defined in Appendix 3. In the mark type column: 'Adult' stands for adult SBW; 'Juvenile' for juvenile SBW.

					Stage – Males							Stage – Females						
Station	Snapshot	Stratum	Date	Mark type	1	2	3	4	5	6	7	1	2	3	4	5	6	7
1	1	11	1-Sep-22	Adult	6	0	1	1	0	0	0	3	1	9	0	0	0	0
2	1	2	1-Sep-22	Juveniles	12	0	0	0	0	0	0	8	0	0	0	0	0	0
3	1	3S	7-Sep-22	Adult	1	15	10	4	0	0	0	1	5	49	0	0	0	0
4	1	4	7-Sep-22	Juveniles	14	0	0	0	0	0	0	12	0	0	0	0	0	0
5	1	5	9-Sep-22	Juveniles	119	0	0	0	0	0	0	93	0	0	0	0	0	0
6	2	7S	12-Sep-22	Adult	0	0	5	10	20	1	0	0	1	49	2	0	0	0
7	2	7S	13-Sep-22	Adult	0	12	26	14	129	0	0	0	0	28	1	0	0	0
8	2	2	17-Sep-22	Adult	1	12	19	6	19	39	77	2	27	9	3	0	2	25
9	2	2	17-Sep-22	Juveniles	144	3	0	0	1	1	0	127	1	0	0	0	0	1
10	2	5	18-Sep-22	Juveniles	10	0	0	0	0	0	0	10	0	0	0	0	0	0
11	2	5	19-Sep-22	Juveniles	69	0	0	0	0	0	0	37	0	0	0	0	0	0
12	2	12	19-Sep-22	Adult	0	3	2	6	49	10	2	0	2	7	47	53	23	7

Table 7: Biomass estimates (in tonnes) and associated coefficient of variation (CV, %) for juvenile, immature, and adult southern blue whiting by stratum and snapshot for the 2022 acoustic survey of the Campbell Island Rise.

	Immature		Immature		Adult	
Stratum	Biomass (t)	CV	Biomass (t)	CV	Biomass (t)	CV
Snapshot 1						
11	0	–	0	–	0	–
2	1 728	54	812	68	23 067	55
3N	0	–	0	–	0	–
3S	0	–	0	–	815	268
4	2 459	38	2 096	51	19 288	41
5	2 586	10	4 025	20	1 700	38
6N	0	–	0	–	1 693	75
6S	0	–	0	–	2 297	118
7N	4 748	29	0	–	6 204	101
7S	28	155	0	–	19 846	80
8E	0	–	0	–	9 787	18
8N	0	–	0	–	0	–
8S	0	–	0	–	3 222	0
Total	11 549	17	6 933	21	87 919	26
Snapshot 2						
11	222	96	174	96	4 929	60
12	0	–	0	–	1 982	46
2	1 970	51	373	63	13 095	39
3S	0	–	0	–	3 097	21
4	5 320	35	676	57	15 064	23
5	3 238	54	1 343	102	11 002	65
6	0	–	0	–	10 692	34
7N	1 987	63	1 213	96	1 145	102
7S	1 243	49	0	–	28 910	88
8	0	–	0	–	6 101	54
Total	13 980	22	3 779	49	96 016	29
Average	12 764	14	5356	22	91 968	20

Table 8: Final biomass summary by sub-areas for adult southern blue whiting on the 2022 acoustic survey of the Campbell Island Rise. Biomass is in tonnes with their associated coefficient of variation (%) in parentheses.

	Snapshot 1	Snapshot 2	Average
All	87 919 (26)	96 016 (29)	91 968 (20)
Core	74 910 (31)	83 005 (33)	78 957 (23)
North	44 870 (34)	47 187 (21)	46 028 (20)
East	16 999 (20)	18 775 (26)	17 887 (17)
South	26 050 (65)	30 055 (85)	28 053 (55)

Table 9: Time series of biomass estimates (in tonnes) and associated coefficient of variation (CV, %) for juvenile, immature, and adult southern blue whiting from acoustic surveys of the Campbell Island Rise. Values for surveys for 1993–2011 are from Fu et al. (2013) and all were calculated using estimates of TS from O'Driscoll et al. (2013).

	Juvenile	CV (%)	Immature	CV (%)	Adult	CV (%)
1993	0	–	35 208	25	16 060	24
1994	0	–	8 018	38	72 168	34
1995	0	–	15 507	29	53 608	30
1998	322	45	6 759	20	91 639	14
2000	423	39	1 864	24	71 749	17
2002	1 969	39	247	76	66 034	68
2004	639	67	5 617	16	42 236	35
2006	504	38	3 423	24	43 843	32
2009	0	–	24 479	26	99 521	27
2011	0	–	14 454	17	53 299	22
2013	0	–	8 004	55	65 801	25
2016	775	37	4 456	19	97 117	16
2019	0	–	4 060	18	91 145	27
2022	12 764	14	5 356	22	91 968	20

Table 10: Time series of spatial distribution of the average biomass of adult SBW (in percentage) from the Campbell Island Rise acoustic surveys between 2009 and 2022. The eastern area was identified as having a separate spawning aggregation of adult southern blue whiting in 2011.

Year	Northern	Southern	Eastern
2009	76.0	24.0	NA
2011	25.8	3.4	70.8
2013	75.1	0	24.9
2016	43.8	11.3	44.9
2019	23.2	51.9	24.9
2022	50.0	30.5	19.4

8. Figures

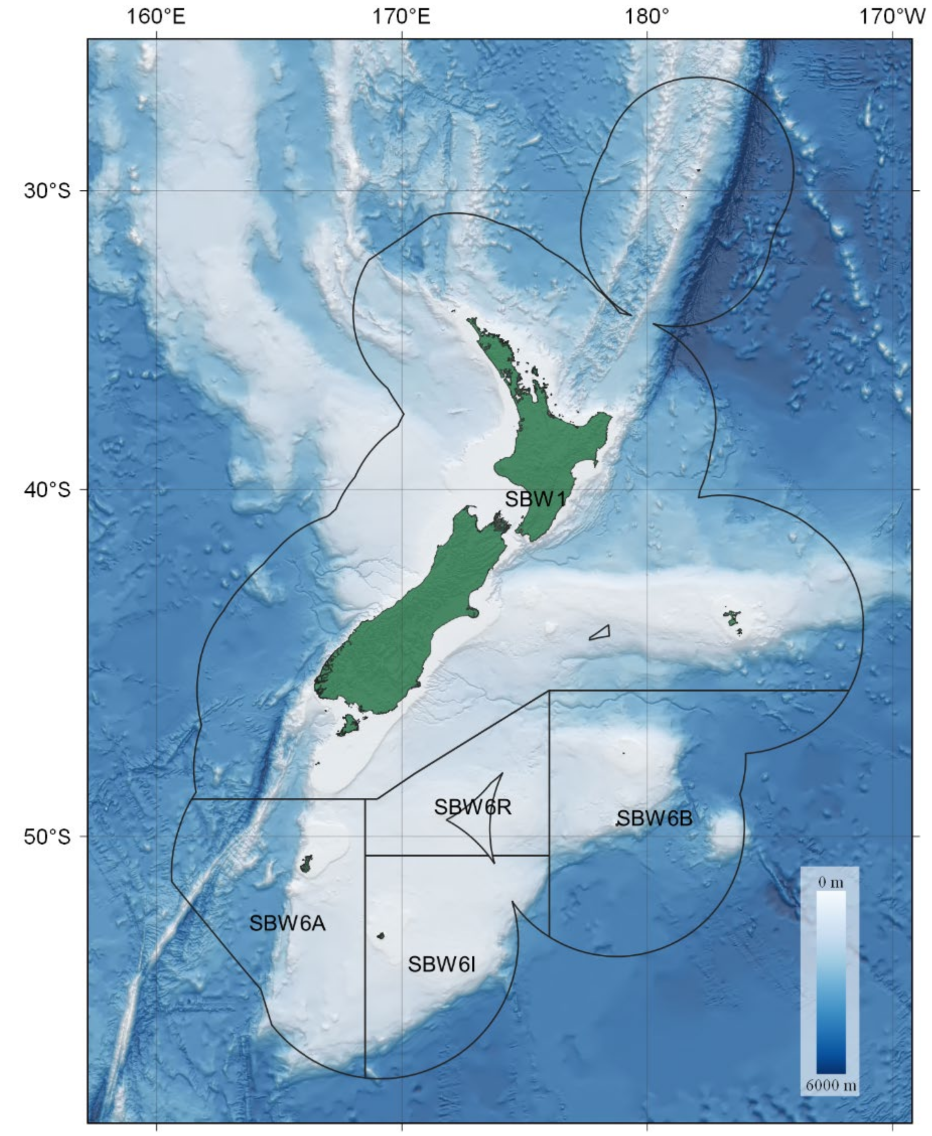

Figure 1: Southern blue whiting Quota Management Areas: New Zealand (excluding Sub-Antarctic, SBW 1), Bounty Platform (SBW 6B), Pukaki Rise (SBW 6R), Auckland Islands Shelf (SBW 6A), and Campbell Island Rise (SBW 6I).

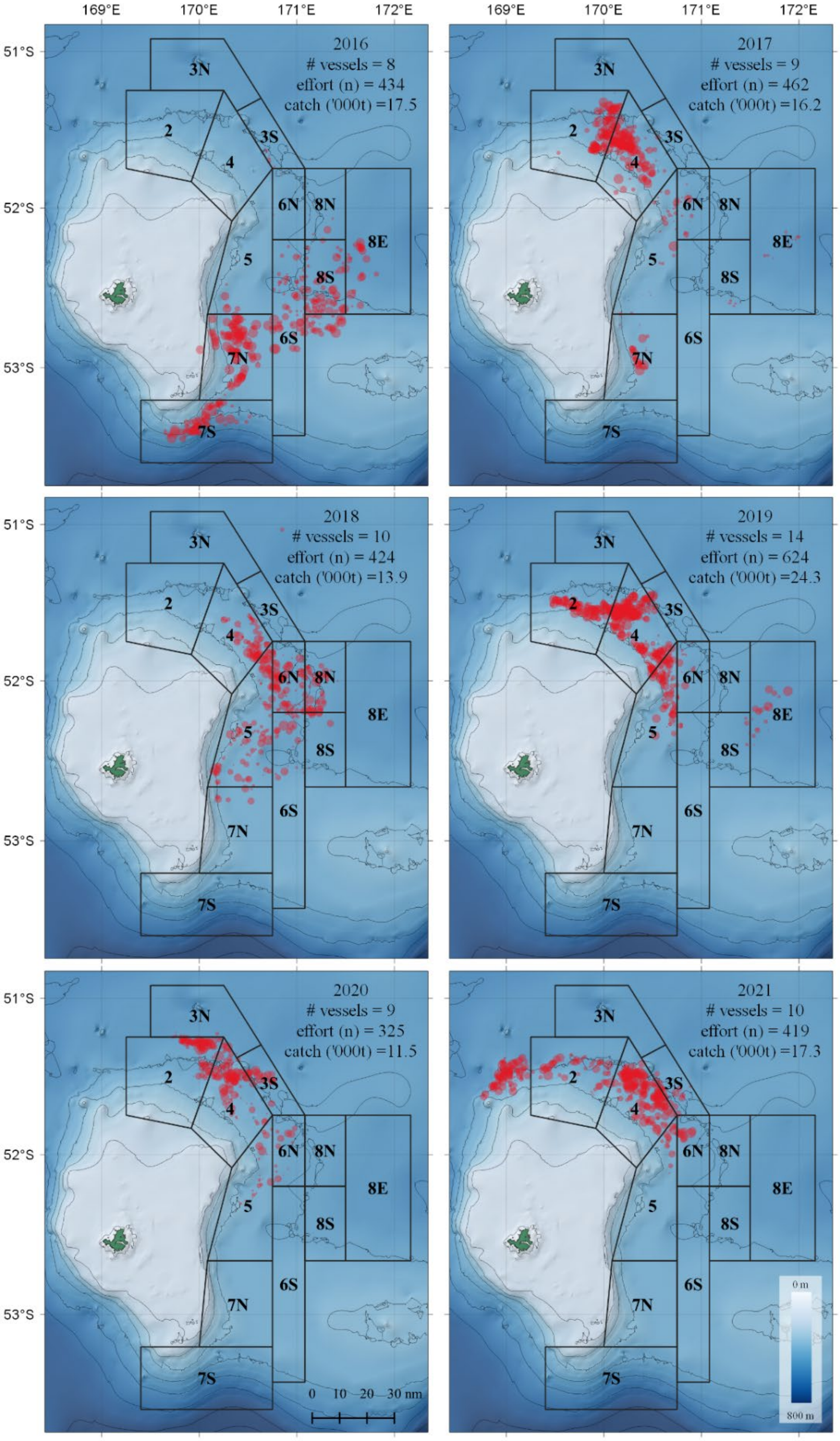

Figure 2: Spatial distribution of catches from commercial trawls on the Campbell Island Rise from 2016 to 21. Circle area is proportional to SBW catch (max. circle area = 200 t). Polygons are stratum boundaries as defined for snapshot 1 of the two previous surveys (i.e., 2016 and 2019). Depth contours are every 100 m.

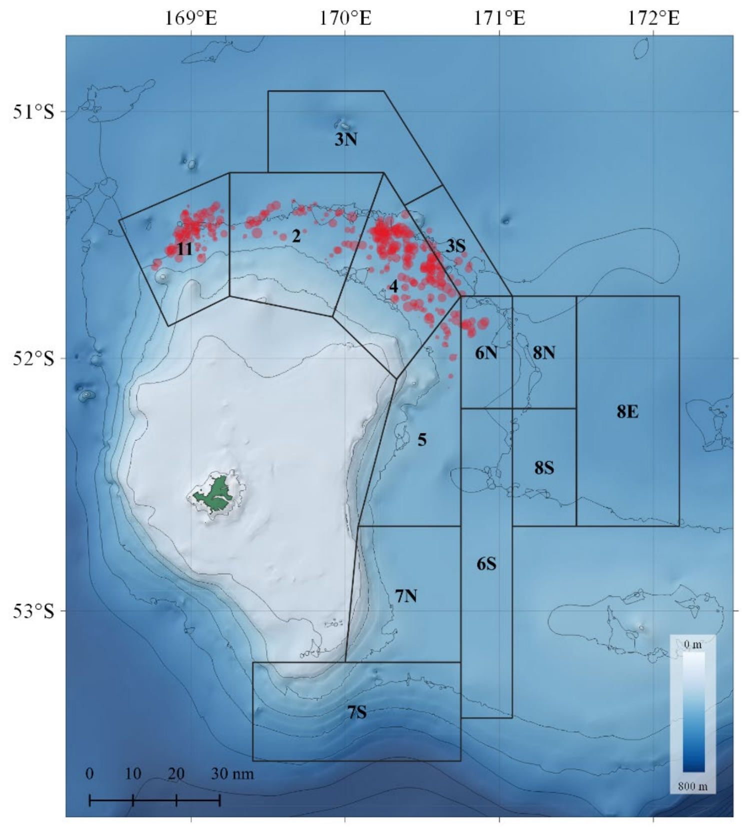

Figure 3: Distribution of commercial catch on the Campbell Island Rise in 2021 and proposed stratum boundaries for snapshot 1 of the 2022 acoustic survey of the Campbell Island Rise. Depth contours are every 100 m.

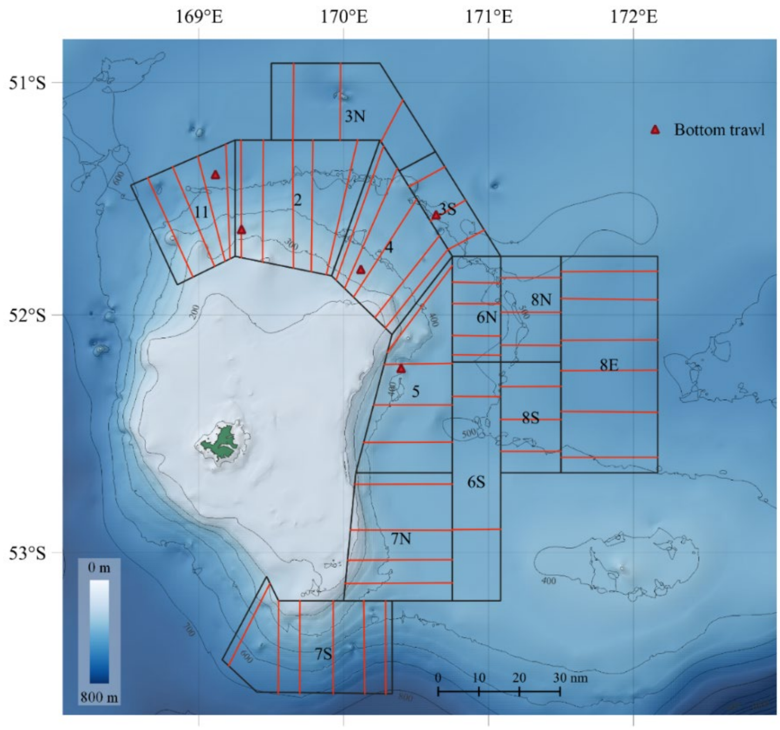

Figure 4: Final stratum definition and indicative transect locations during the snapshot 1 of the 2022 acoustic survey of southern blue whiting on Campbell Island Rise (TAN2210). A total of thirteen strata were surveyed, with a total number of 52 transects (orange lines). Five mark identification trawls (all bottom trawls) were carried out.

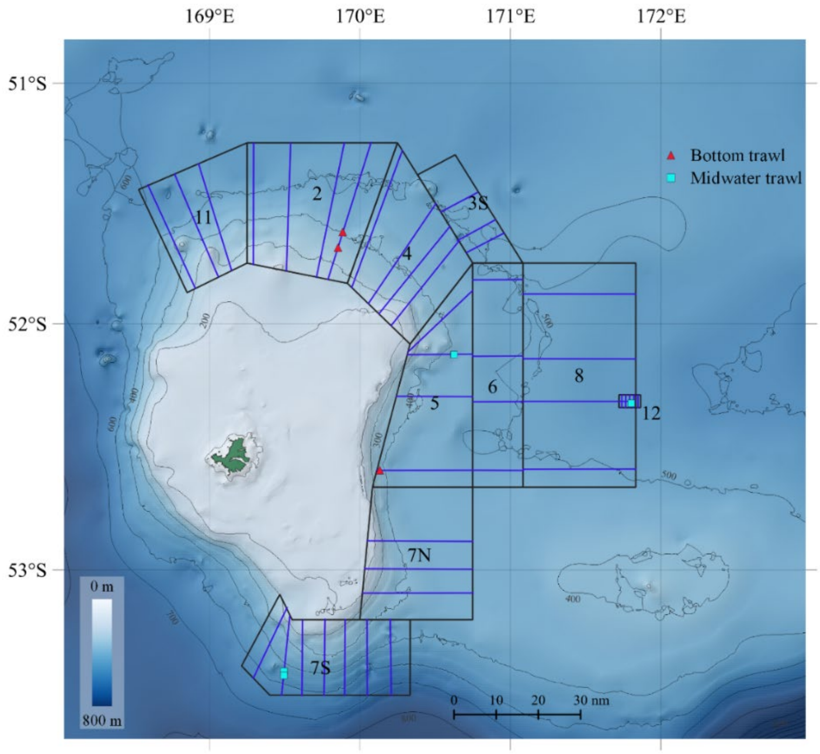

Figure 5: Final stratum definition and indicative transect locations during the snapshot 2 of the 2022 acoustic survey of southern blue whiting on Campbell Island Rise (TAN2210). A total of nine strata were surveyed, with a total number of 41 transects (blue lines). Seven mark identification trawls (four midwater and three bottom trawls) were carried out.

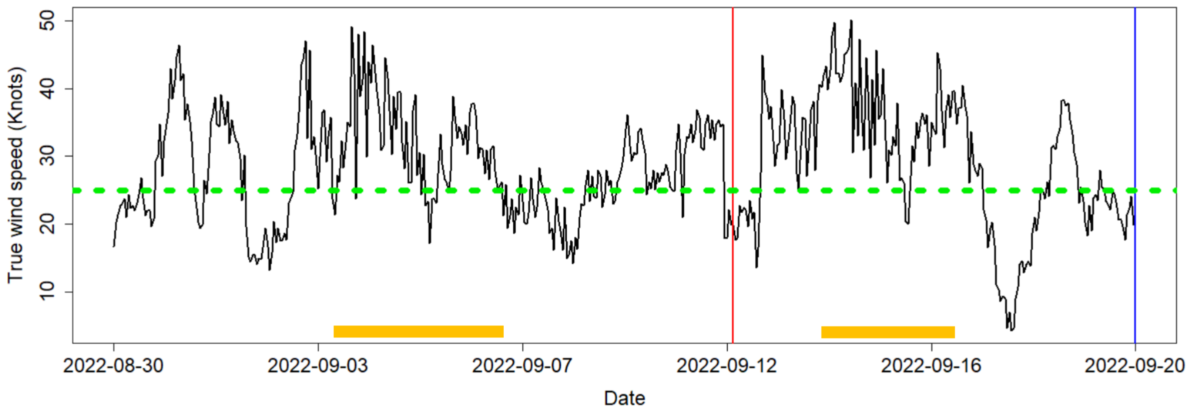

Figure 6: Output from *Tangaroa* data acquisition system (DAS) showing mean hourly wind speed (in knots) during the survey. Data are true wind speed, i.e., corrected for relative motion of ship. Red vertical line indicates the end of the first snapshot and start of the second. Blue line indicates the completion of the second snapshot. Green dashed line at 25 knots is considered the maximum threshold for collection of acoustic data with hull-mounted transducers. Orange bars indicate periods of sheltering east of Campbell Island.

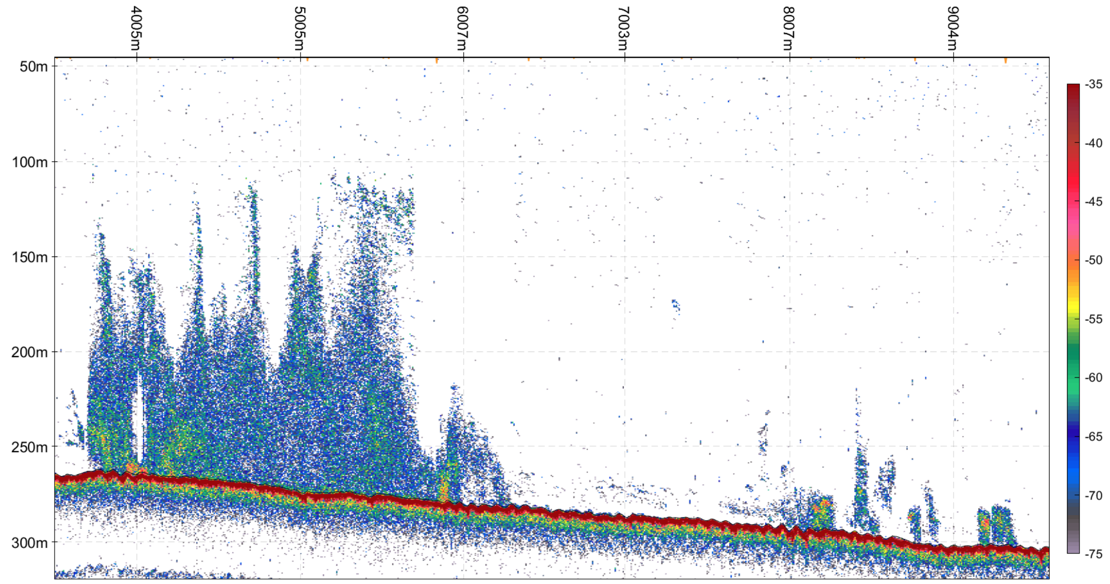

Figure 7: Echogram showing aggregations of juvenile southern blue whiting detected in snapshot 1. Aggregations were detected during the day on transect number 1 in stratum 5. X-axis shows distance (m) and y-axis shows range (m) from the dual frequency towed body (DuFT) towed at 50 m depth. Data were collected using the DuFT at 38 kHz.

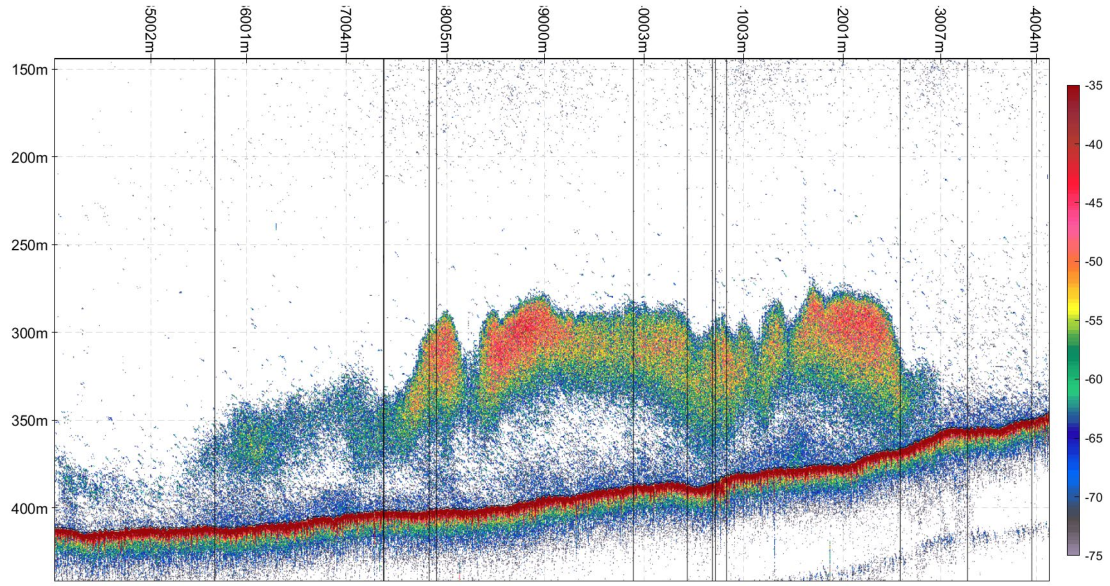

Figure 8: Echogram showing a pre-spawning aggregation of southern blue whiting found at dusk on transect number 5 in stratum 2, during snapshot 1. X-axis shows distance (m) and y-axis shows range (m) from the dual frequency towed body (DuFT) towed at 50 m depth. Data were collected using the DuFT at 38 kHz.

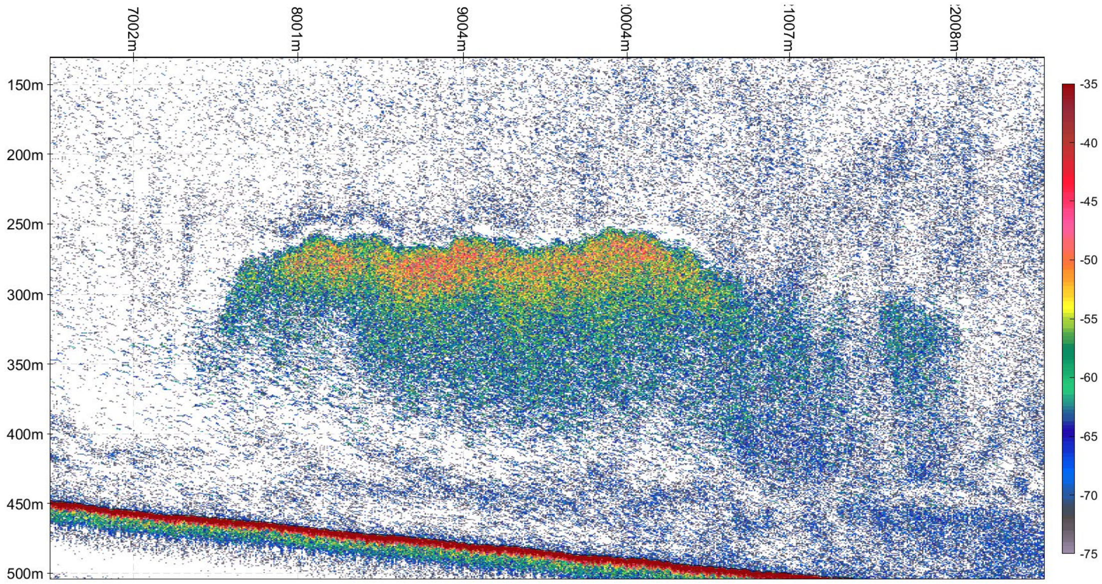

Figure 9: Echogram showing a pre-spawning aggregation of adult southern blue whiting from snapshot 1. Aggregation was detected at night on transect number 2 (west–east direction) in stratum 7S. X-axis shows distance (m) and y-axis shows range (m) from the dual frequency towed body (DuFT) towed at 50 m depth. Data were collected using the DuFT at 38 kHz.

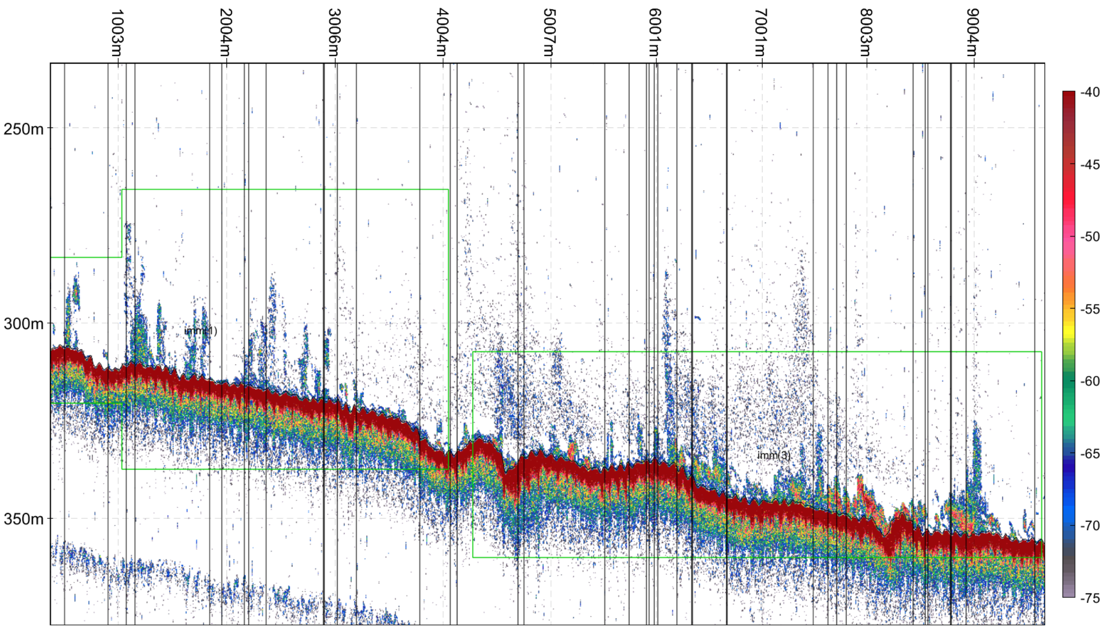

Figure 10: Echogram showing an aggregation of immature southern blue whiting from snapshot 1. Aggregation was detected during daytime on transect number 1 (north–south direction) in stratum 5. X-axis shows distance (m) and y-axis shows range (m) from the dual frequency towed body (DuFT) towed at 50 m depth. Data were collected using the DuFT at 38 kHz.

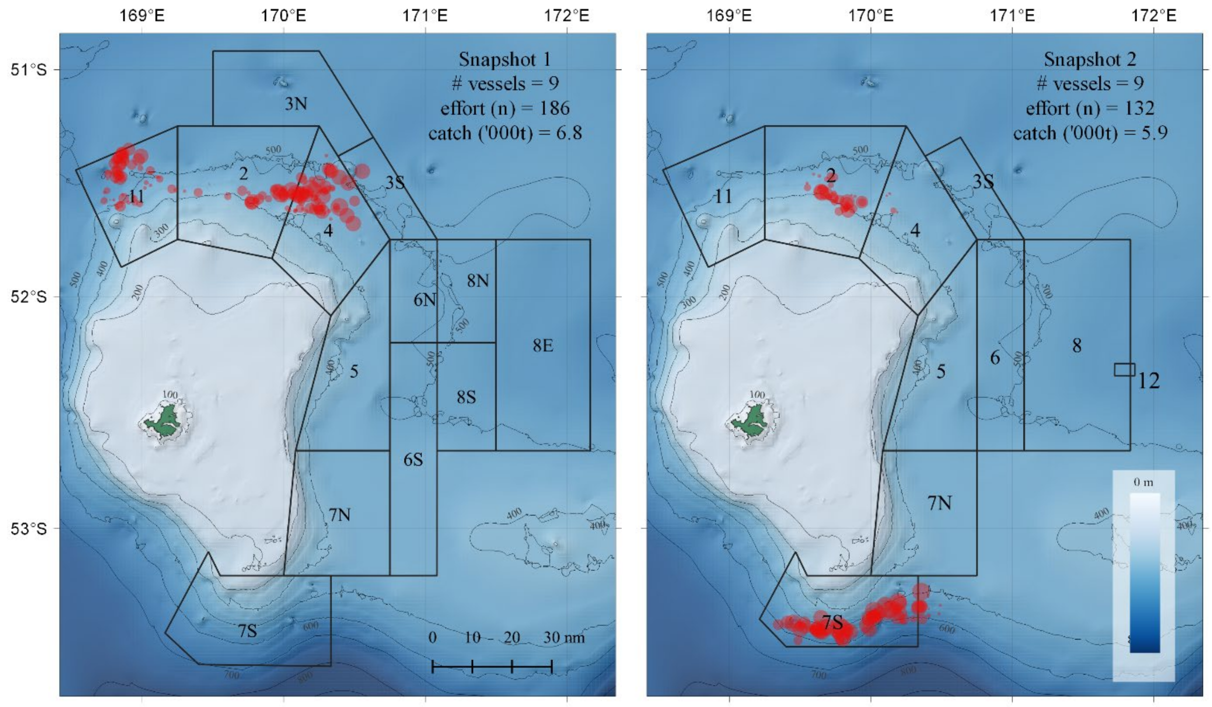

Figure 11: Distribution of commercial catch during the 2022 acoustic survey of the Campbell Island Rise Snapshot 1 was completed between 30 August and 11 September (left panel) and snapshot 2 was completed between 12 and 20 September (right panel). Circle area is proportional to SBW catch rate. Max. circle area = 160 t.

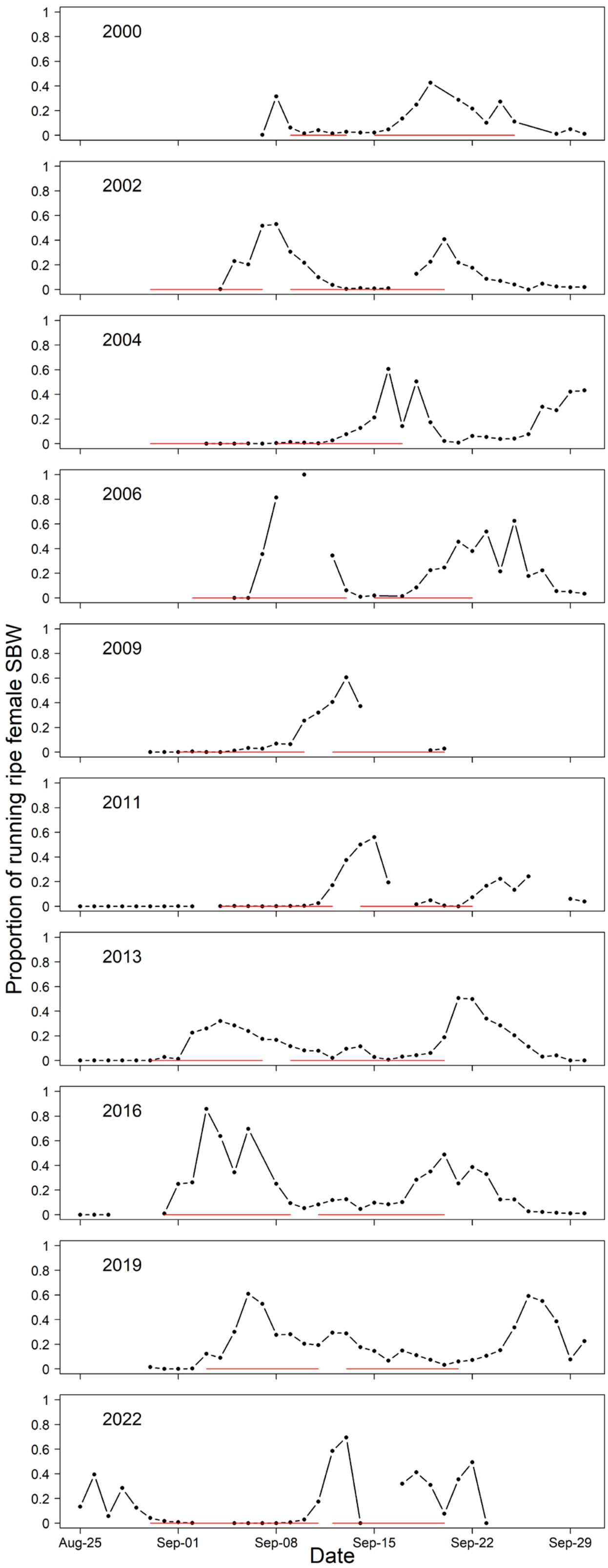

Figure 12: Survey timing (red line above x axis) in relation to the timing of spawning for the acoustic surveys from 2000 to 2022 on the Campbell Island Rise. Proportion of running ripe females is from observer data.

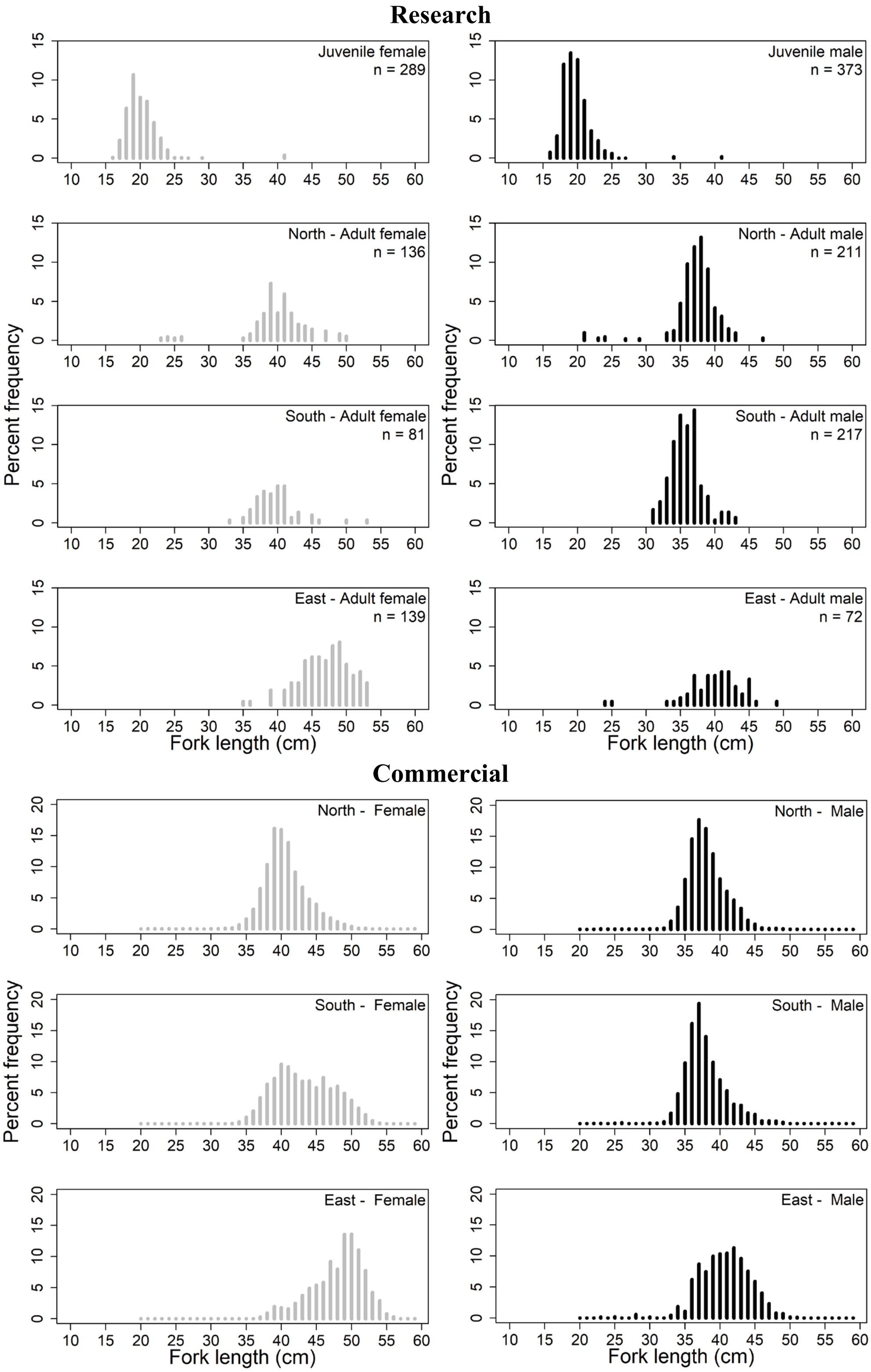

Figure 13: Catch-weighted length frequency distributions for southern blue whiting caught in research mark identification trawls during the 2022 acoustic survey (top panels), and from commercial tows during the spawning fishery (bottom panels). SBW are separated as juvenile or adult in research trawls. For adults, size distributions were separated into North (strata 11, 2, 3N, 3S, 4, 5), East (strata 6N, 6S, 6, 8N, 8S, 8E, 8, and 12), and South (strata 7N and 7S). The *n* values for research trawls show number of males and females measured.

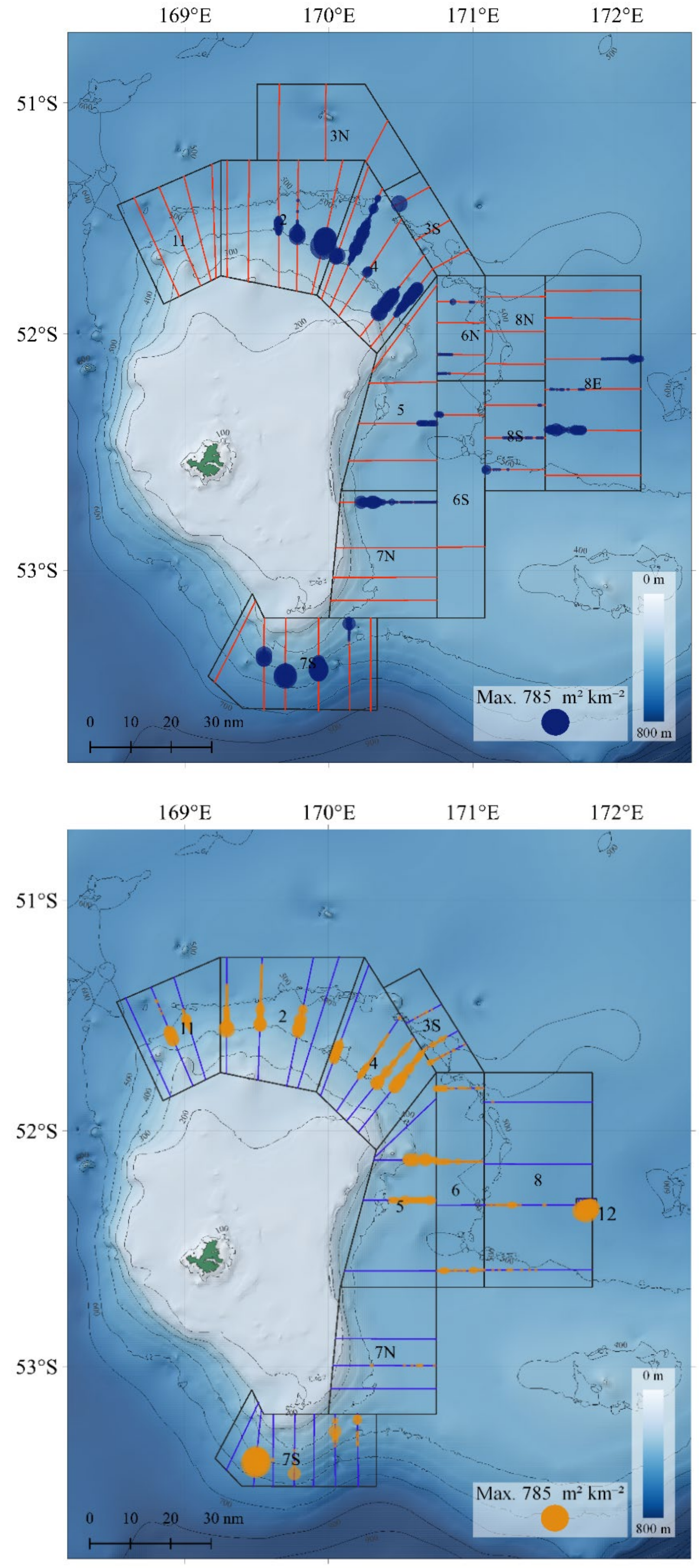

Figure 14: Spatial distribution of acoustic backscatter from adult SBW (averaged over 10 consecutive pings, i.e., approximately 100 m) for snapshots 1 (top) and 2 (bottom). Circle area is proportional to acoustic backscatter.

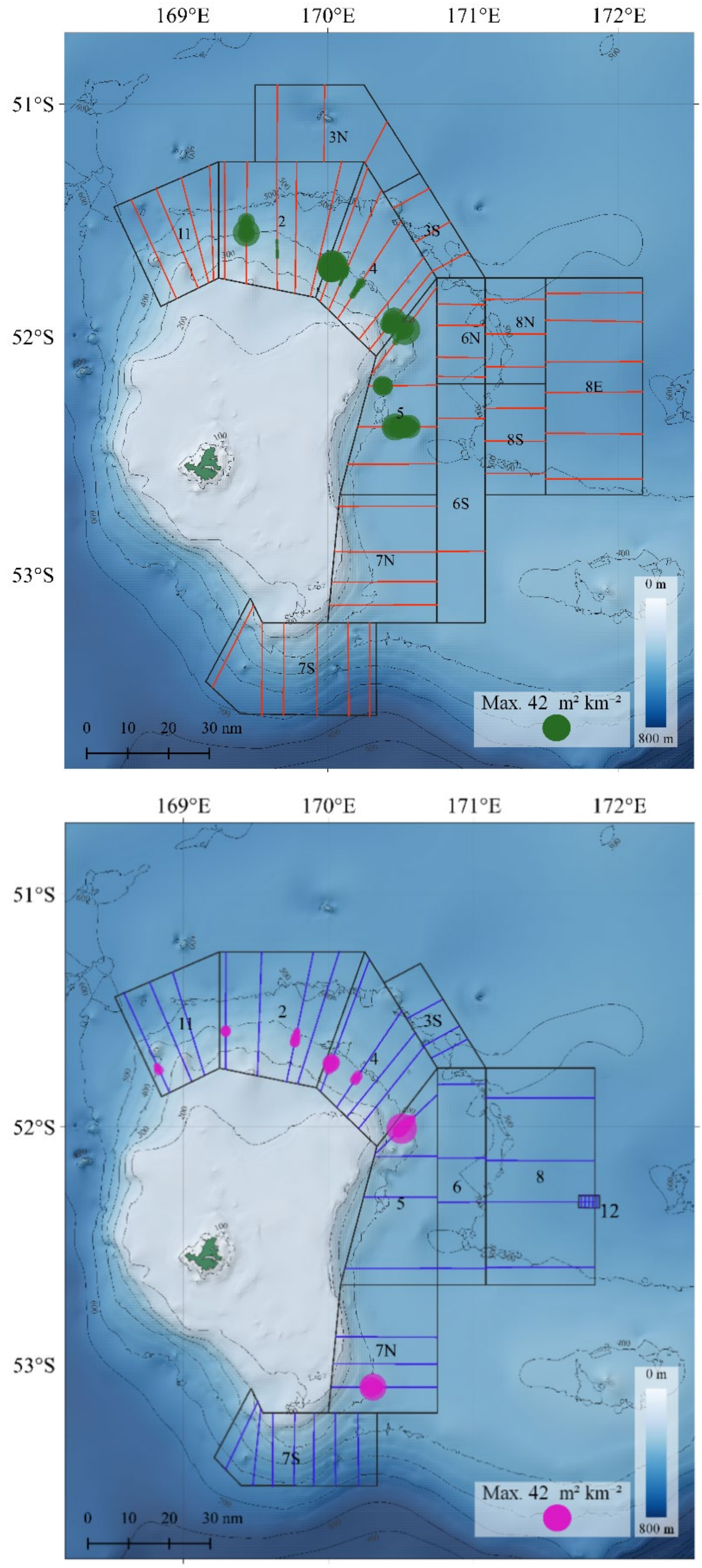

Figure 15: Spatial distribution of acoustic backscatter from immature SBW (averaged over 10 consecutive pings, i.e., approximately 100 m) for snapshots 1 (top) and 2 (bottom). Circle area is proportional to acoustic backscatter.

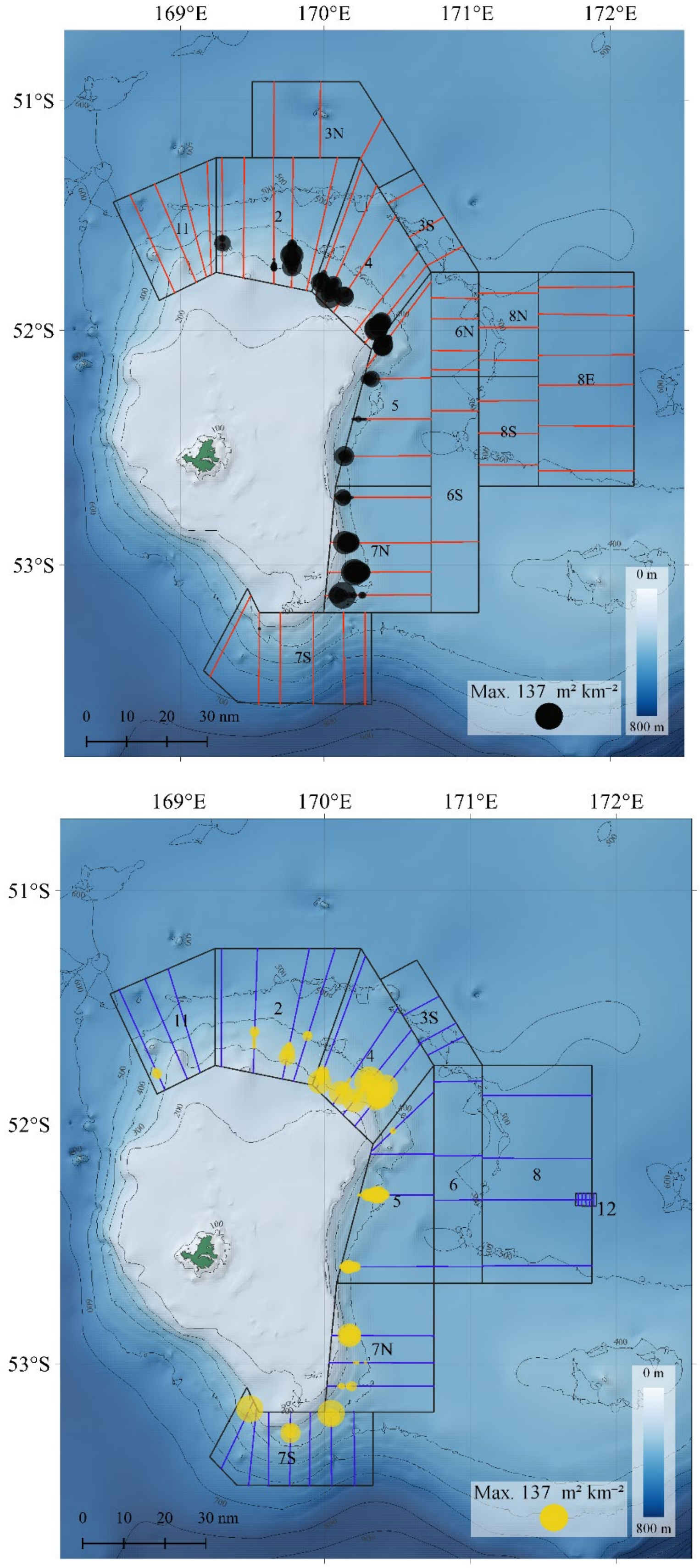

Figure 16: Spatial distribution of acoustic backscatter from juvenile SBW (averaged over 10 consecutive pings, i.e., approximately 100 m) for snapshots 1 (top) and 2 (bottom). Circle area is proportional to acoustic backscatter.

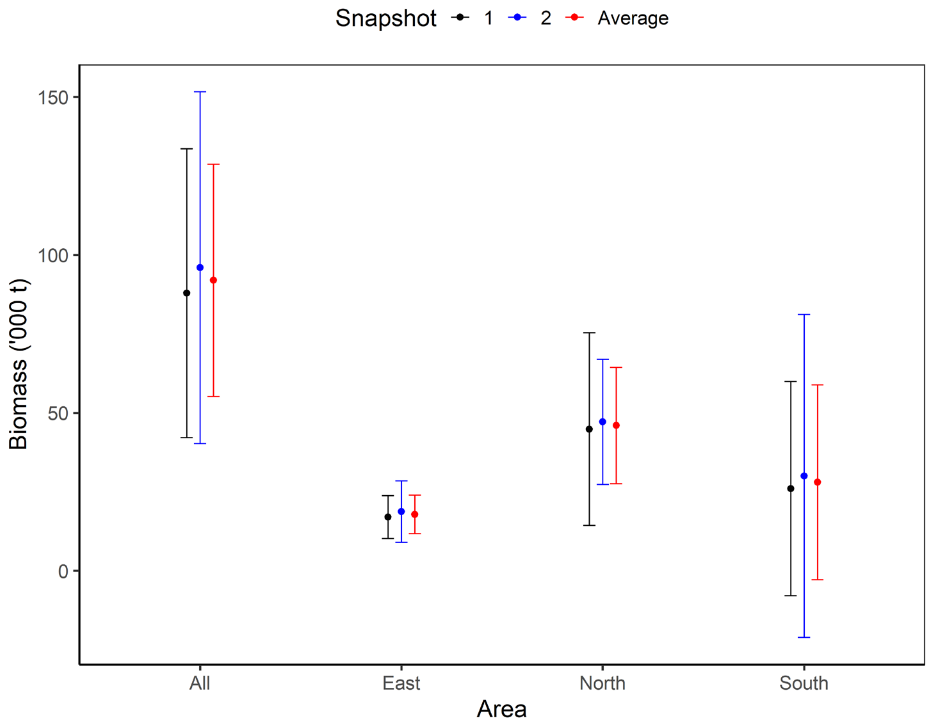

Figure 17: Comparison of snapshot 1 and 2 biomass estimates and their average for adult SBW, categorised by general area, for the 2022 Campbell acoustic survey. Error bars are ± 2 standard errors.

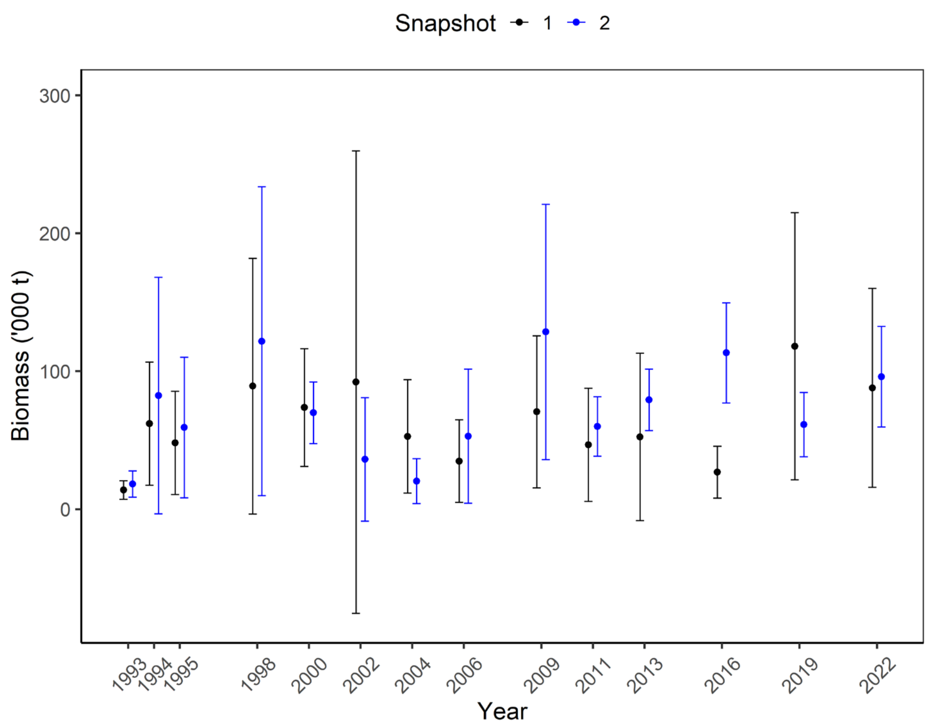

Figure 18: Comparison of snapshot 1 and 2 biomass estimates for adult SBW for all Campbell acoustic surveys up to 2022. Error bars are ± 2 standard errors. Values for surveys for 1993–2011 are from Fu et al. (2013) and all were calculated using estimates of TS from O'Driscoll et al. (2013).

APPENDIX 1: Calibration report RV *Tangaroa* hull-mounted EK60/EK80 echosounder systems

The echosounders on RV *Tangaroa* were calibrated on 28 August 2022 north of Banks Peninsula (43˚ 12.35’ S, 172˚ 01.63’ E), at the start of the acoustic survey of southern blue whiting stock on Campbell Island Rise (TAN2210). The calibration was conducted broadly as per the procedures of Demer et al. (2015). The echosounder configuration consisted of three EK60 (38, 120, and 200 kHz) and two EK80 (18 and 70 kHz) systems. The EK80 systems were calibrated in continuous wave (CW) and frequency modulated (FM) or broadband mode using 2.048 ms (12–27 and 50–90 kHz) and 4.096 ms (12–27 kHz). The transceiver settings used during the calibration are shown in Table A1. 1.

A weighted line was passed under the keel to facilitate setting up the three lines and calibration sphere. Long (3.8 m) fibreglass calibration poles were used to help keep the calibration lines clear of the hull. The sphere and associated lines were immersed in a soap solution prior to entering the water. A lead weight was deployed about 6 m below the sphere to steady the arrangement of lines.

The weather the during the calibration was good with 10 knots of south-easterly wind and 1 m swell. Initially the calibration was attempted with the vessel drifting (‘unclutched’); however, as the vessel was drifting at speed of about 1 knot, the decision to anchor was made.

The calibration started at 14:30 NZST on 28 August, and the sphere was first located in the beam at 15:59 on 28 August. The CW calibration was done first. At the start of the calibration the sphere was positioned around the centre of the beam of the 38 kHz transducer to obtain data for the on-axis calibration. Because of vessel movement the sphere moved within the beam of its own accord. Due to the close proximity of all five transducers, a number of echoes were recorded across all frequencies. During the calibration the sphere was moved to ensure on-axis calibrations and good coverage of the beam patterns of all frequencies. Once the CW calibration was complete (16:50) the recording was stopped and the transceivers settings changed for FM calibrations. The first FM calibrations started at 16:51, which were done using 2.049 ms pulse length. The sphere was positioned near the centre of the beam of the 18 and 70 kHz transducer and then was moved around to ensure good on-axis and beam pattern coverage. The first FM calibrations were completed at 17:11. The final calibration started immediately after and it was done using 4.096 ms pulse length for which the sphere was centred on the beam of the 18 kHz transducer. The calibration was completed at 17:35 on 28 August.

The calibration data were recorded using EK80 software in raw file format: TAN2210-D20220828-T035916.raw (CW calibration), TAN2210-D20220828-045143 and TAN2210-D20220828-051118 (2.048 ms pulse length at 18kHz FM calibrations), and TAN2210-D20220828-051418 (4.096 ms pulse length at 18kHz FM). These data are stored in the NIWA *acoustics* database. The EK60 transceiver settings in effect during the calibration are given in Table A1. 1.

A temperature/salinity/depth profile was taken using a Seabird SBE37-SM (V 2.6b Serial No. 2958) conductivity, temperature, and depth probe (CTD). Estimates of acoustic absorption were calculated using the formulae of Doonan et al. (2003). The formula from Francois & Garrison (1982) was used at 200 kHz. Estimates of seawater sound speed and density were calculated using the formulae of Fofonoff & Millard (1983). The sphere target strength was calculated as per equations 6 to 9 of MacLennan (1981), using longitudinal and transverse sphere sound velocities of 6853 and 4171 m s^{-1} respectively and a sphere density of 14 900 kg m^{-3}.

Analysis

The data in the .raw EK80 files were extracted using the software ESP3 (Ladroit et al. 2020). The amplitude of the sphere echoes was obtained by filtering on range and choosing the sample with the highest amplitude. Instances where the sphere echo was disturbed by fish echoes were discarded. The alongship and athwartship beam widths and offsets were calculated by fitting the sphere echo amplitudes to the Simrad theoretical beam pattern:

$$compensation = 6.0206\left(\left(\frac{2\theta_{fa}}{BW_{fa}}\right)^2 + \left(\frac{2\theta_{ps}}{BW_{ps}}\right)^2 - 0.18\left(\frac{2\theta_{fa}}{BW_{fa}}\right)^2\left(\frac{2\theta_{ps}}{BW_{ps}}\right)^2\right),$$

where θ_{ps} is the port/starboard echo angle, θ_{fa} the fore/aft echo angle, BW_{ps} the port/starboard beamwidth, BW_{fa} the fore/aft beamwidth, and *compensation* the value, in dB, to add to an uncompensated echo to yield the compensated echo value. The fitting was done using an unconstrained nonlinear optimisation (as implemented by the Matlab `fminsearch` function). The S_a correction was calculated from:

$$Sa, corr = 5\log 10\left(\frac{\sum P_i}{4P_{\max}}\right),$$

where P_i is sphere echo power measurements and P_{max} the maximum sphere echo power measurement. A value for $S_{a,corr}$ is calculated for all valid sphere echoes and the mean over all sphere echoes is used to determine the final $S_{a,corr}$.

Results

The results from the CTD cast are given in Table A1. 2, along with estimates of the sphere target strength, sound speed, and acoustic absorption for 18, 38, 70, 120, and 200 kHz.

The calibration parameters resulting from the CW calibrations are given in Table A1. 3 and compared with results from previous calibrations (since 2015). Excluding calibrations carried out in Antarctica, the results from calibrations at 38 kHz have been relatively consistent (usually within 0.5 dB). Calibrations in Antarctic have also been consistent between themselves. The results from calibrations for the higher frequencies (120 and 200 kHz) were more variable over time.

The estimated beam patterns, as well as the coverage of the beam by the calibration sphere, are given in Figures A1. 1–10. The symmetrical nature of the beam patterns and the centreing near zero indicates that the transducers and transceivers were all operating correctly.

The root mean square (RMS) of the difference between the Simrad beam model and the sphere echoes out to the 3 dB beamwidth was 0.13 dB for 18 kHz, 0.12 for 38 kHz, 0.18 dB for 70 kHz, 0.16 dB for 120 kHz, and 0.20 dB at 200 kHz (Table A1. 3), indicating excellent quality calibrations for 18–120 kHz and good quality calibration for 200 kHz (<0.4 dB is acceptable, 0.2-0.3 dB good, and <0.2 dB excellent). On-axis estimates were derived from 280 sphere echoes at 18 kHz, 132 echoes at 38 kHz, 51 echoes at 70 kHz, 55 echoes at 120 kHz, and 122 echoes at 200 kHz.

Results of the broadband calibrations showed a change of beamwidth with frequency that matched the theoretical curves (see Figures A1. 11–13). The gain for the 18 kHz WBT showed strong changes over the bandwidth, which was expected given the narrow band of the transducer used. The consistency of TS measurement (see bounds in Figure A.1 11) showed a consistent behaviour of the transducer in the 12–27 kHz frequency band. The 70 kHz WBT curves matched the theoretical curves closely over most of the used band.

References

Demer, D.A., Berger, L., Bernasconi, M., Bethke, E., Boswell, K., Chu, D., Domokos, R., et al. (2015). Calibration of acoustic instruments. *ICES Cooperative Research Report No. 326*. 133 p.

Doonan, I.; Coombs, R.; McClatchie, S. (2003). The absorption of sound in seawater in relation to estimation of deep-water fish biomass. *ICES Journal of Marine Science 60*: 1047–1055.

Fofonoff, P.; Millard, R., Jr (1983). Algorithms for computation of fundamental properties of seawater. *UNESCO Technical Papers in Marine Science 44*. 53 p.

Francois, R.E.; Garrison, G.R. 1982. Sound absorption based on ocean measurements. Part II: Boric acid contribution and equation for total absorption. *Journal of the Acoustical Society of America 72*: 1879–1890.

Knudsen, H.P. (2009) Long-term evaluation of scientific-echosounder performance. *ICES Journal of Marine Science 66*: 1335–1340.

Ladroit, Y.; Escobar-Flores, P.C.; Schimel, A.C.G.; O'Driscoll, R.L. (2020). ESP3: An opensource software for the quantitative processing of hydro-acoustic data. *SoftwareX 12*: 100581

MacLennan, D.N. (1981). The theory of solid spheres as sonar calibration rargets. *Scottish Fisheries Research 22*. 17 p.

Table A1. 1: EK60/EK80 transceiver settings and other relevant parameters in effect during the calibration.

Parameter					
Frequency (kHz)	18	38	70	120	200
GPT model	--	0090720580ea	--	009072058148	00907205da23
GPT/WBT serial number	400065	650	145607	668	692
GPT/WBT software version	2.54	70413.0	2.54	70413.0	70413.0
EK80 software version	21.15.1	21.15.1	21.15.1	21.15.1	21.15.1
Transducer model	ES18-11	ES38B	ES70-7C	ES120-7C	ES200-7C
Transducer serial number	2080	31378	158	477	364
Sphere type/size	tungsten carbide/38.1 mm diameter (same for all frequencies)				
Transducer draft setting (m)	0.0	0.0	0.0	0.0	0.0
Transmit power (W)	1000	2000	750*	250*	150*
Pulse length (ms) CW/FM	1.024/2.048 & 4.096	1.024	1.024/2.048	1.024	1.024
Transducer peak gain by pulse length (dB)	22.40/22.40 & 23.0	25.50	25.5/25.5	27.0	26.0
Sa correction (dB)	0.00	0.00	0.00	0.00	0.00
Bandwidth (Hz)	0	0	0	0	0
Sample interval (ms) by pulse length (dB)	0.052/0.043 & 0.052	0.256	0.048/0.016	0.256	0.256
Two-way (equivalent) beam angle (dB)	–17.0	–20.7	–20.7	–20.7	–20.7
Angle sensitivity (dB) along/athwartship	15.50/15.50	23.0/23.0	23.0/23.0	23.0/23.0	23.0/23.0
3 dB beamwidth (º) along/athwartship	11.0/11.0	7.0/7.0	7.0/7.0	7.0/7.0	7.0/7.0
Angle offset (º) along/athwartship	0.0/0.0	0.0/0.0	0.0/0.0	0.0/0.0	0.0/0.0

* Maximum transmit power of 70, 120, and 200 kHz echosounders was reduced when ER60 software was upgraded in April 2013. Previously transmit power was 1000 W, 500 W, and 300 W respectively.

Table A1. 2: TD cast details and derived water properties. The values for sound speed, salinity, and absorption are the mean over water depths 6 to 30 m.

Parameter	
Date/time (NZST, start)	28 August 2022 17:45
Position	43˚ 12.35’ S, 172˚ 01.63’ E
Mean sphere range (m)	29.6 (18 kHz), 29.8 (38), 29.4 (70), 29.7 (120), 29.7 (200)
Mean temperature (ºC)	9.9
Mean salinity (psu)	34.0
Sound speed (m/s)	1489.2
Water density (kg/m^3)	1026.7
Sound absorption (dB/km)	2.49 (18 kHz) 9.42(38 kHz) 22.33 (70 kHz) 37.16 (120 kHz) 53.39 (200 kHz)
Sphere target strength (dB re 1 m^2)	–42.71 (18 kHz) –42.39 (38 kHz) –41.28 (70 kHz) –39.48 (120 kHz) –39.25 (200 kHz)

Table A1. 3: **Estimated calibration coefficients for all calibrations of *Tangaroa* hull EK80 (continuous wave - CW)/EK60 echosounders since 2015. Transducer peak gain was estimated from mean sphere TS. * The 38 kHz transducer was changed in October 2015. The Jan 2021, 2019, and Feb 2015 calibrations were in Antarctica. Calibrations of the 18 and 70 kHz echosounders in 2021 and 2019 are from EK80 systems. (Continued next page)**

		Aug 2022	Jan 2021	Aug 2019	Jan 2019	Jul 2018	Aug 2016	Feb 2016	Feb 2015
18 kHz	Transducer peak gain (dB)	23.36	N/A	22.92	23.43	N/A	22.80	22.85	23.21
	Sa correction (dB)	-0.168	N/A	-0.76	-0.76	N/A	-0.71	-0.73	-0.76
	Beamwidth (º) along/athwartship	10.45/10.34	N/A	9.7/9.7	9.7/9.7	N/A	10.6/10.9	10.5/11.3	10.7/11.2
	Beam offset (º) along/athwartship	-0.009/0.033	N/A	-0.04/0.14	-0.04/0.14	N/A	0.00/0.00	0.00/0.00	0.00/0.00
	RMS deviation (dB)	0.13	N/A	0.12	0.12	N/A	0.10	0.14	0.12
38 kHz*	Transducer peak gain (dB)	26.43	26.29	26.31	26.32	26.37	26.23	26.21	25.69
	Sa correction (dB)	-0.60	-0.54	-0.59	-0.56	-0.55	-0.62	-0.58	-0.54
	Beamwidth (º) along/athwartship	6.7/6.8	6.7/6.5	6.8/6.8	6.6/6.6	6.7/6.8	7.0/7.1	6.9/7.2	6.8/6.9
	Beam offset (º) along/athwartship	0.05/-0.12	0.13/0.20	0.06/-0.12	0.11/-0.14	0.06/-0.08	0.00/0.00	0.14/-0.19	0.00/0.00
	RMS deviation (dB)	0.12	0.20	0.08	0.14	0.12	0.11	0.14	0.12
70 kHz	Transducer peak gain (dB)	27.14	N/A	26.36	26.27	N/A	26.33	26.28	26.55
	Sa correction (dB)	-0.16	N/A	-0.33	-0.32	N/A	-0.31	-0.38	-0.35
	Beamwidth (º) along/athwartship	7.1/ 7.2	N/A	6.8/6.8	6.4/6.5	N/A	6.4/6.6	6.2/6.5	6.6/6.7
	Beam offset (º) along/athwartship	-0.23/-0.04	N/A	0.00/0.00	0.02/0.06	N/A	0.00/0.00	0.13/-0.04	0.04/-0.02
	RMS deviation (dB)	0.18	N/A	0.06	0.16	N/A	0.13	0.18	0.10
120 kHz	Transducer peak gain (dB)	25.89	26.01	26.71	26.29	26.20	26.19	26.15	26.92
	Sa correction (dB)	-0.38	-0.26	-0.38	-0.37	-0.45	-0.33	-0.29	-0.33
	Beamwidth (º) along/athwartship	6.6/6.8	6.4/6.4	6.5/6.4	6.4/6.6	6.7/6.8	6.3/6.5	6.1/6.2	6.4/6.5
	Beam offset (º) along/athwartship	-0.09/0.03	0.00/-0.13	-0.10/0.04	-0.01/-0.01	-0.02/0.00	0.00/0.00	-0.00/0.00	-0.00/0.00
	RMS deviation (dB)	0.16	0.23	0.17	0.18	0.20	0.17	0.18	0.16

200 kHz	Transducer peak gain (dB)	25.11	24.67	25.09	24.98	25.15	24.92	25.10	24.90
	Sa correction (dB)	-0.25	-0.32	-0.33	-0.20	-0.29	-0.17	-0.22	-0.27
	Beamwidth (º) along/athwartship	6.7/6.8	6.2/6.4	6.8/6.6	6.3/6.4	6.5/6.5	6.4/6.3	6.2/6.2	6.6/6.9
	Beam offset (º) along/athwartship	-0.08/-0.16	0.22/-0.27	-0.24/-0.08	0.18/-0.08	-0.03/-0.1	0.00/0.00	0.00/0.00	0.00/0.00
	RMS deviation (dB)	0.21	0.26	0.20	0.19	0.25	0.19	0.18	0.20

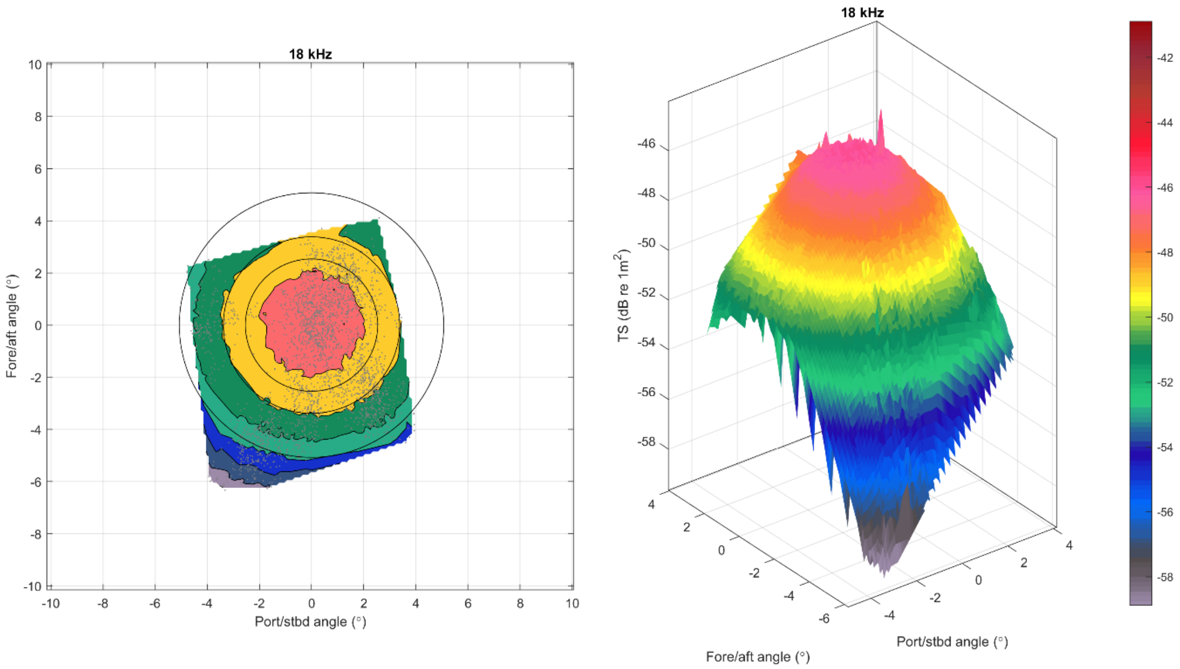

Figure A1. 1: The 18 kHz estimated beam pattern from the sphere echo strength and position shown in two- (left) and three-dimensional (right) coordinate planes. The '+' symbols indicate where sphere echoes were received. The colours indicate the received sphere echo strength in dB re 1 m^2.

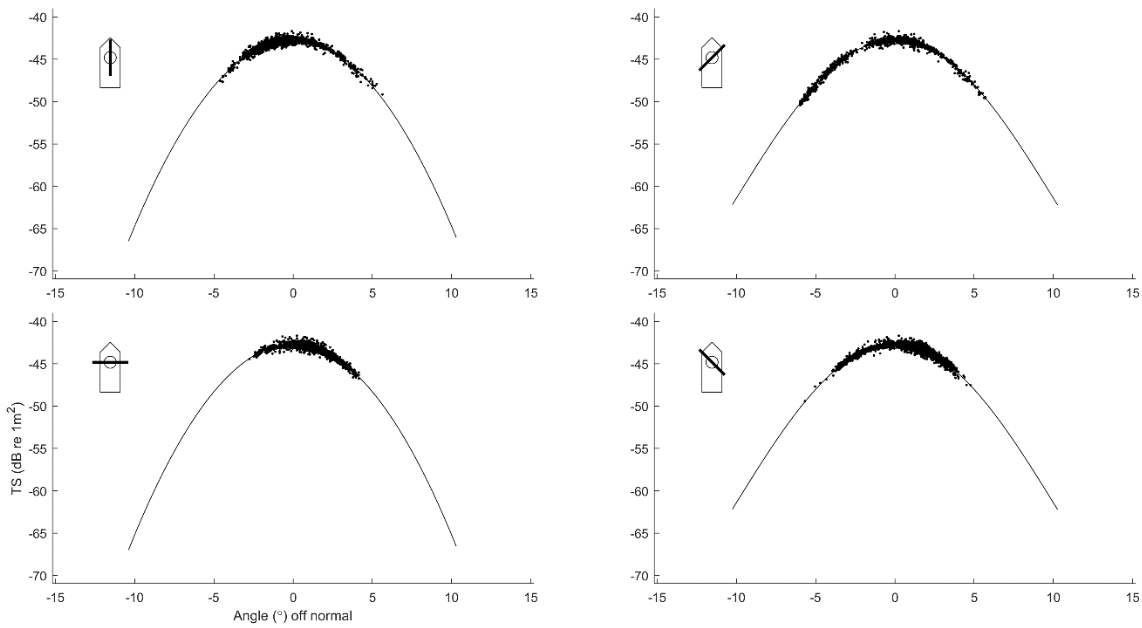

Figure A1. 2: Beam pattern results from the 18 kHz analysis. The solid line is the ideal beam pattern fit to the sphere echoes for four slices through the beam.

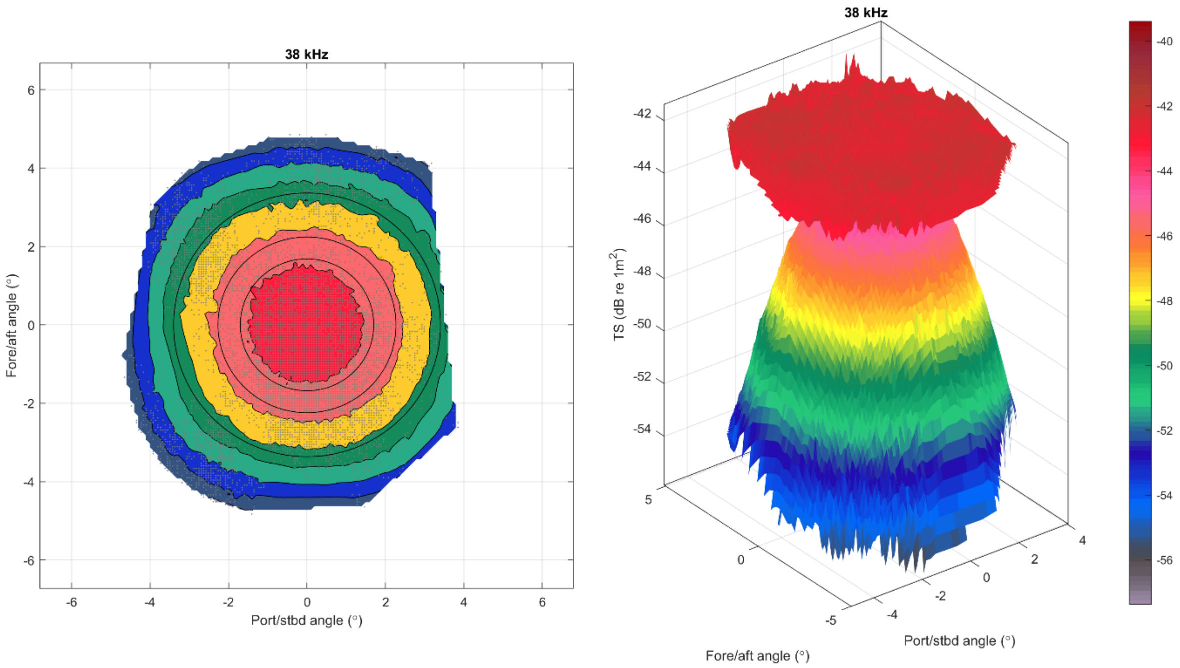

Figure A1. 3: The 38 kHz estimated beam pattern from the sphere echo strength and position shown in two- (left) and three-dimensional (right) coordinate planes. The '+' symbols indicate where sphere echoes were received. The colours indicate the received sphere echo strength in dB re 1 m^2.

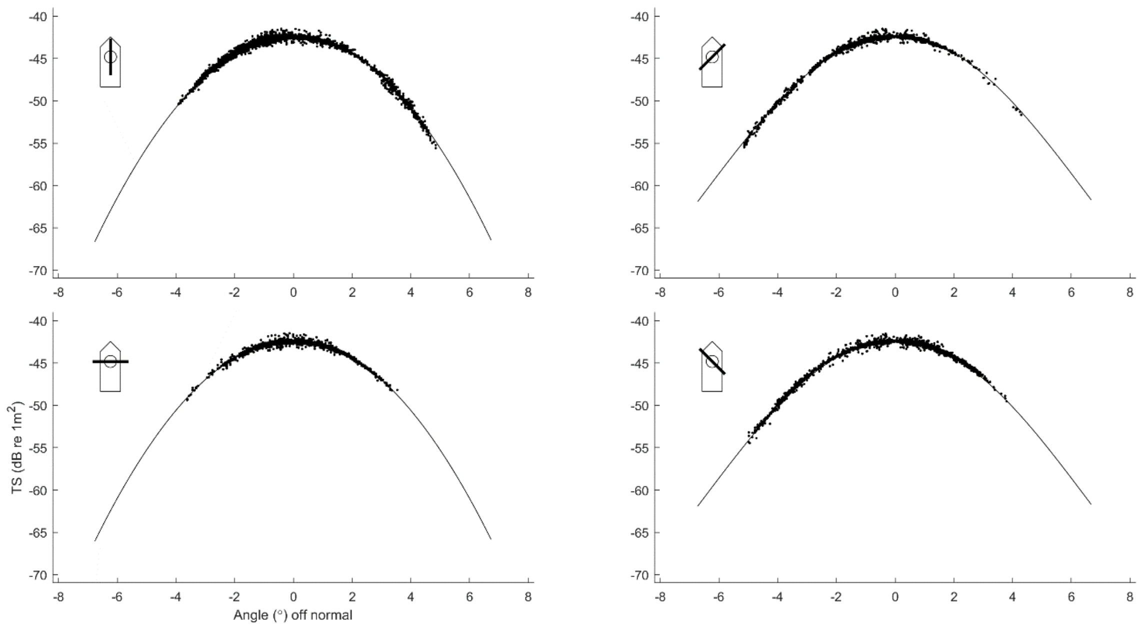

Figure A1. 4: Beam pattern results from the 38 kHz analysis. The solid line is the ideal beam pattern fit to the sphere echoes for four slices through the beam.

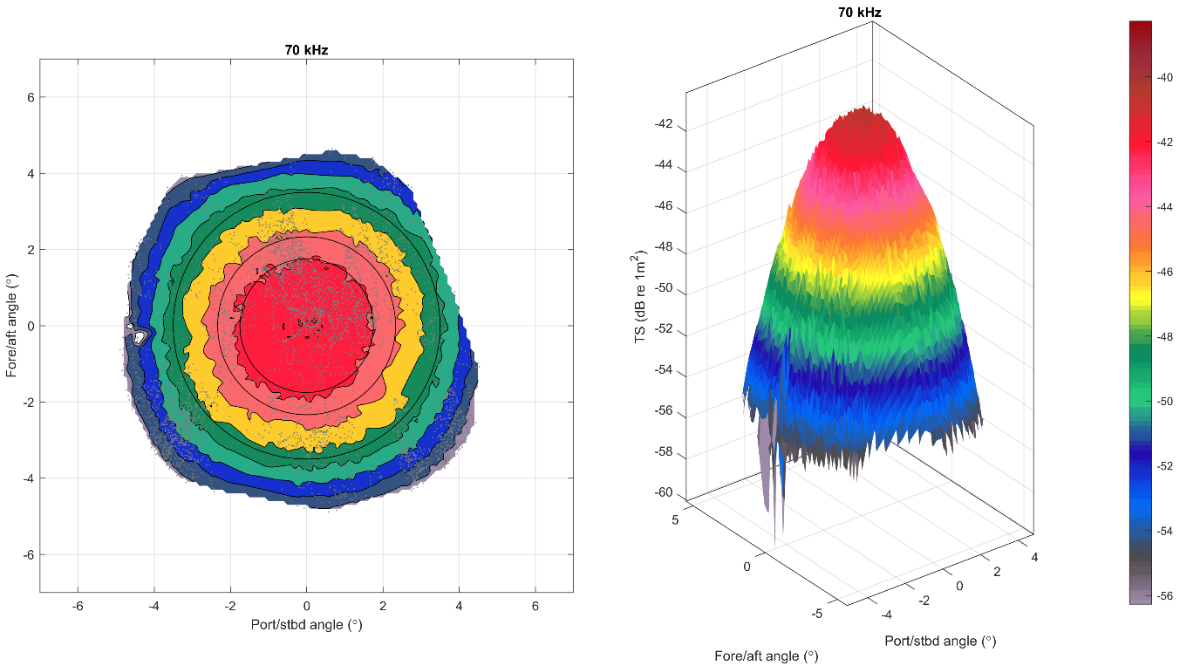

Figure A1. 5: The 70 kHz estimated beam pattern from the sphere echo strength and position shown in two- (left) and three-dimensional (right) coordinate planes. The '+' symbols indicate where sphere echoes were received. The colours indicate the received sphere echo strength in dB re 1 m^2.

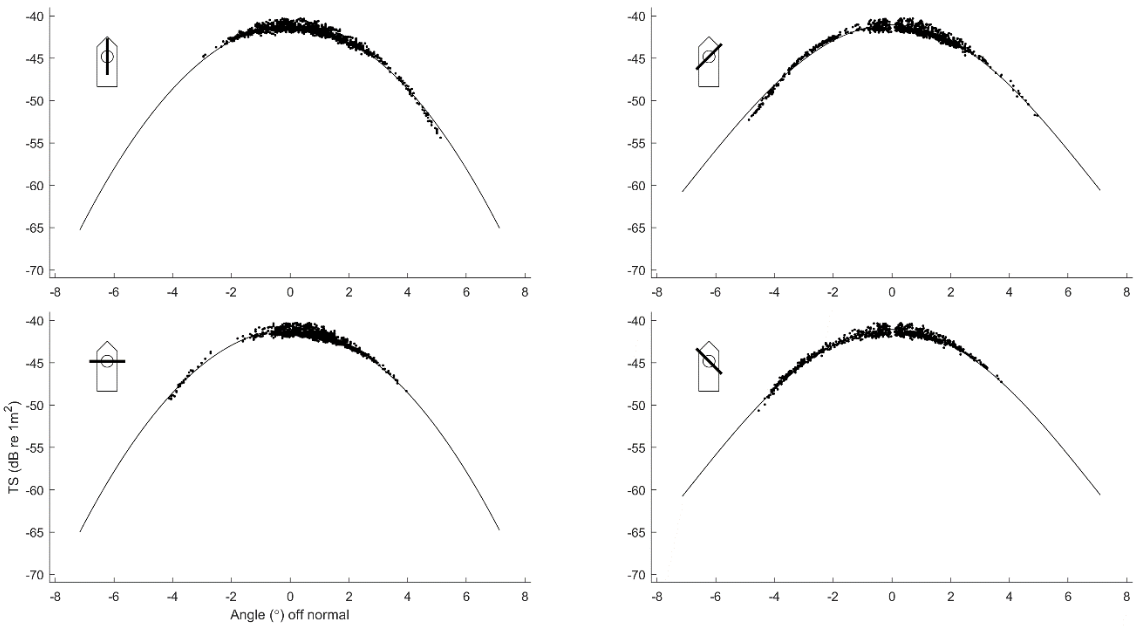

Figure A1. 6: Beam pattern results from the 70 kHz analysis. The solid line is the ideal beam pattern fit to the sphere echoes for four slices through the beam.

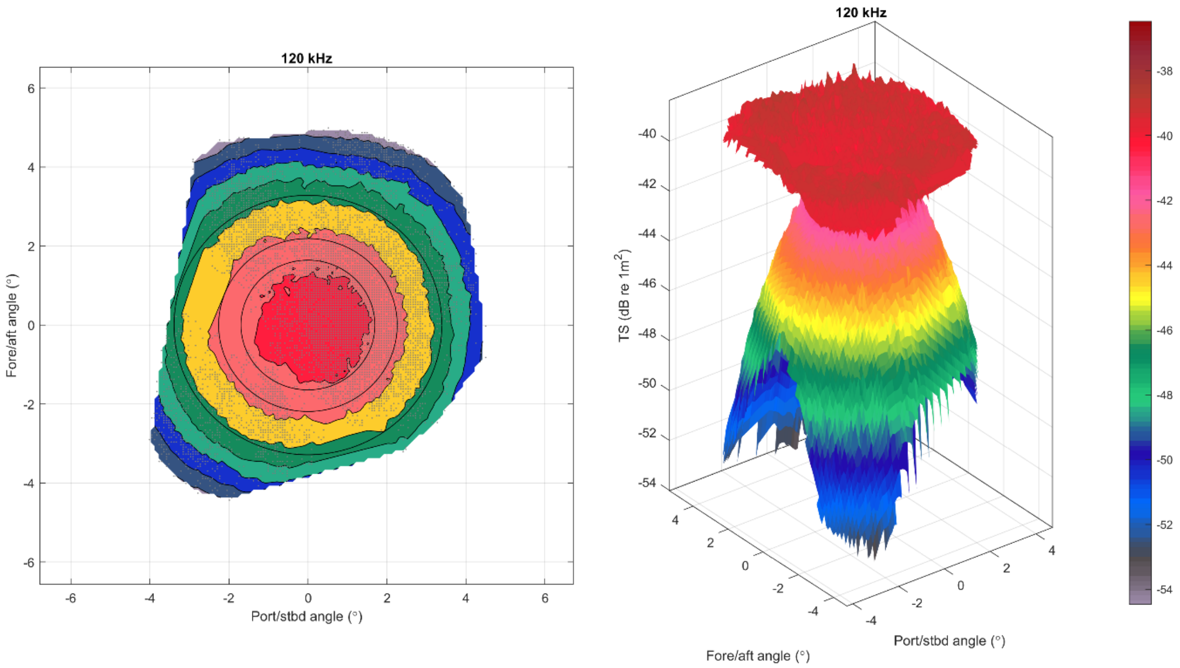

Figure A1. 7: The 120 kHz estimated beam pattern from the sphere echo strength and position shown in two- (left) and three-dimensional (right) coordinate planes. The '+' symbols indicate where sphere echoes were received. The colours indicate the received sphere echo strength in dB re 1 m^2.

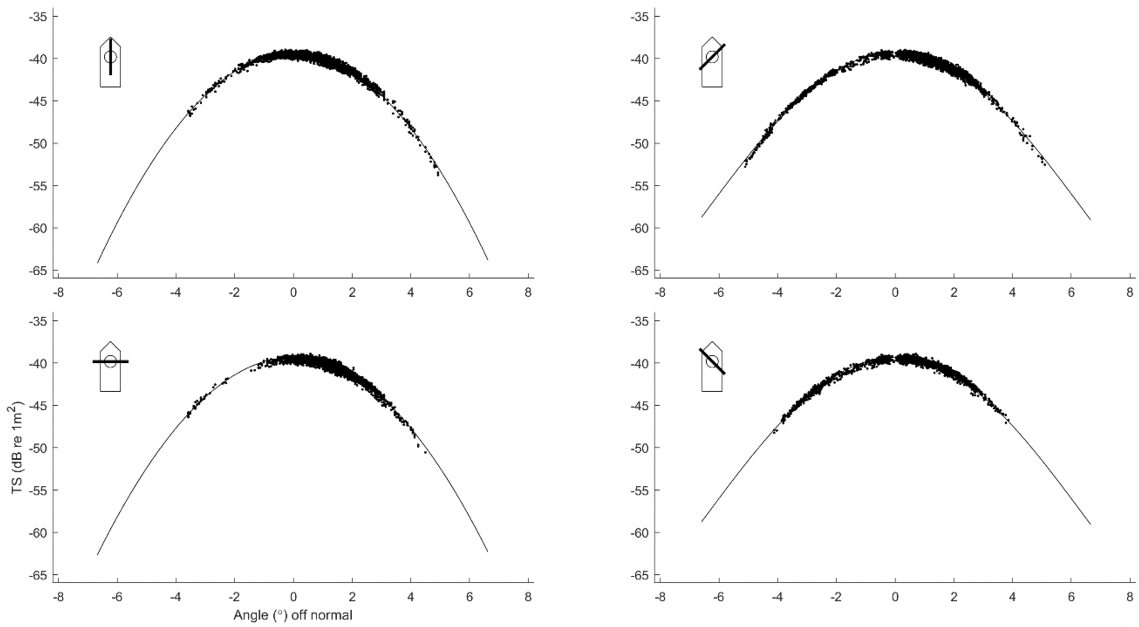

Figure A1. 8: Beam pattern results from the 120 kHz analysis. The solid line is the ideal beam pattern fit to the sphere echoes for four slices through the beam.

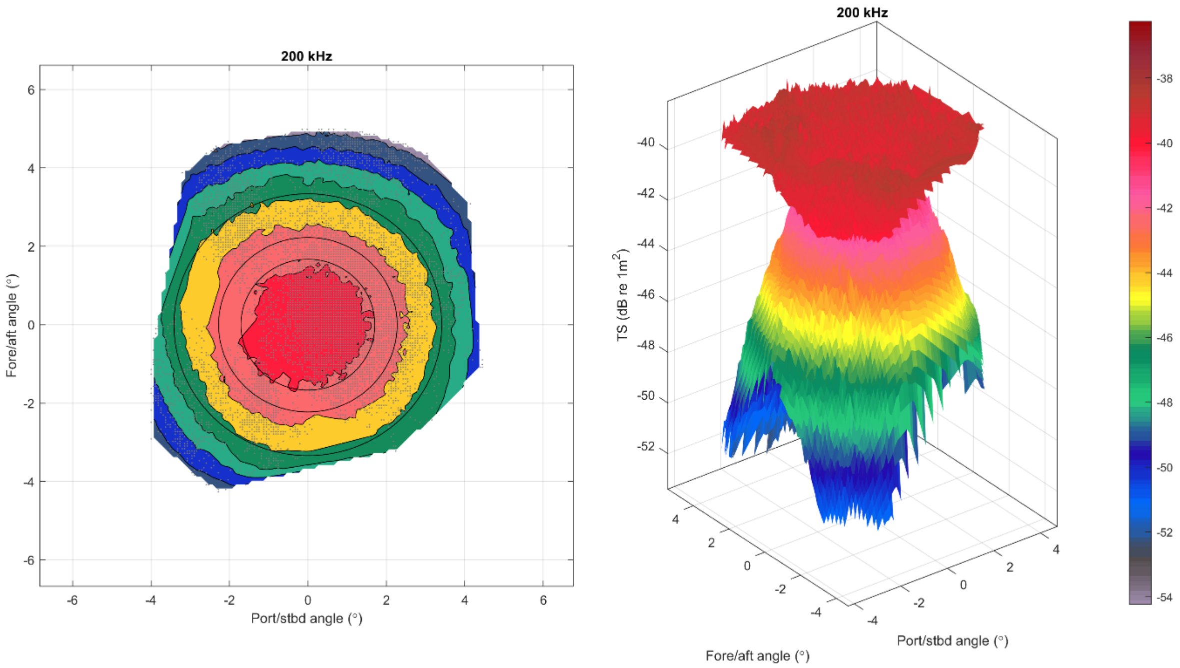

Figure A1. 9: The 200 kHz estimated beam pattern from the sphere echo strength and position shown in two- (left) and three-dimensional (right) coordinate planes. The '+' symbols indicate where sphere echoes were received. The colours indicate the received sphere echo strength in dB re 1 m^2.

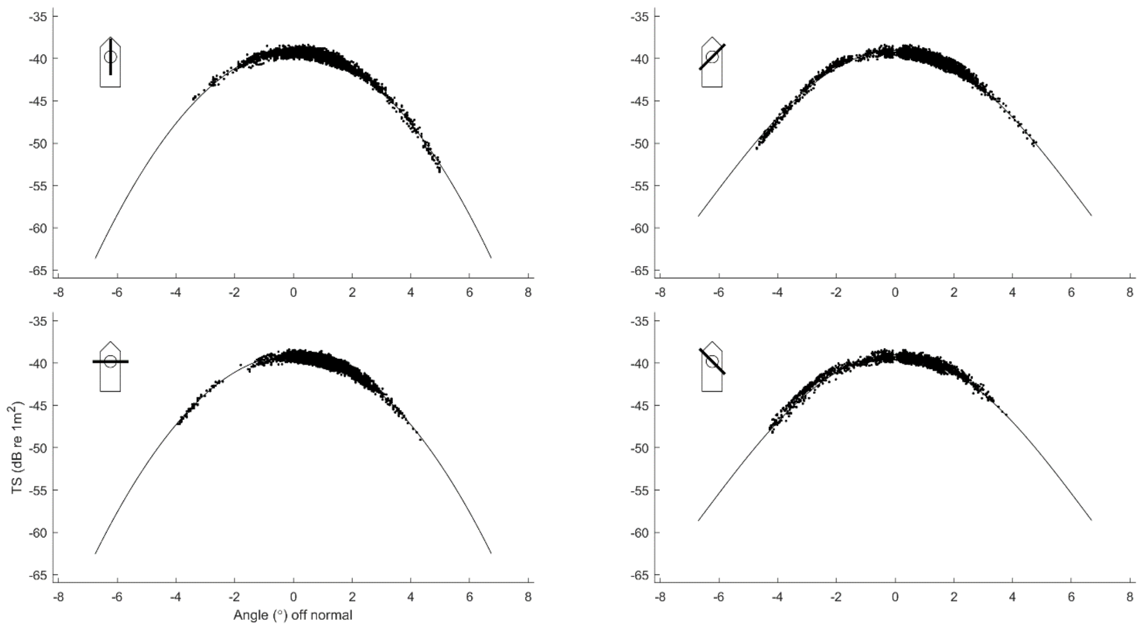

Figure A1. 10: Beam pattern results from the 200 kHz analysis. The solid line is the ideal beam pattern fit to the sphere echoes for four slices through the beam.

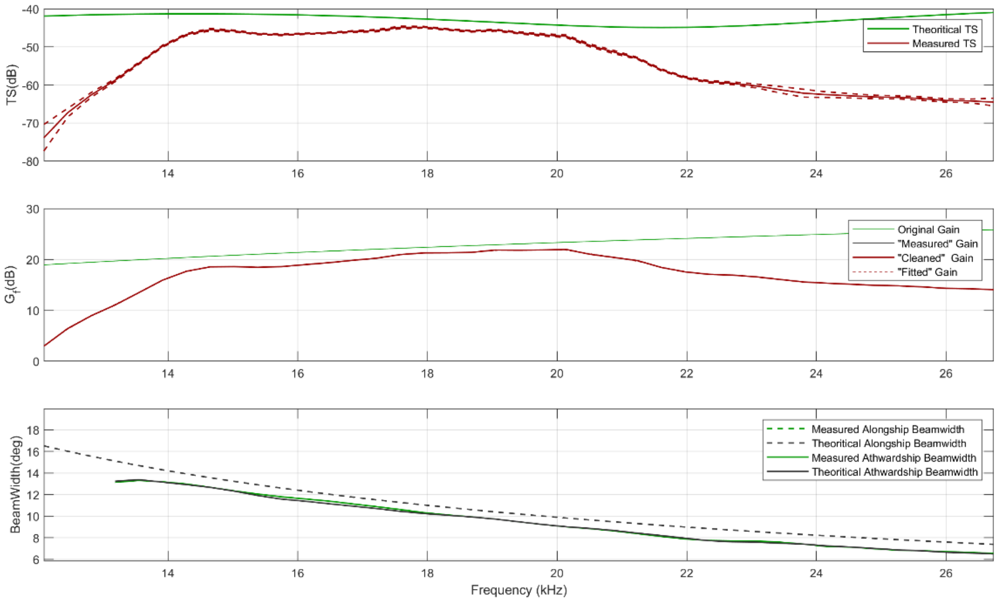

Figure A1. 11: Target strength (in dB re 1 m^2), gain, and beam angle estimation as a function of frequency for the 18 kHz WBT (12-27 kHz) for the calibration done using a pulse length of 2.048 ms. Final usable bandwidth: 12-27 kHz. Top: red dotted lines show the bounds (two times the standard deviation) around the average TS measurements obtained from 186 echoes within 0.30 degrees of the centre of the beam.

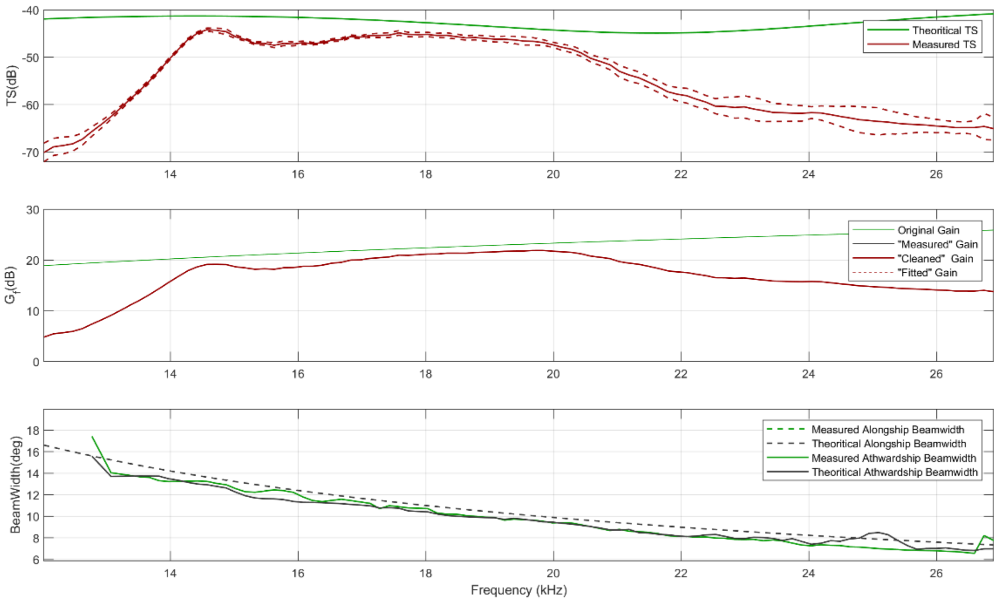

Figure A1. 12: Target strength (in dB re 1 m^2), gain, and beam angle estimation as a function of frequency for the 18 kHz WBT (12-27 kHz) for the calibration done using a pulse length of 4.096 ms. Final usable bandwidth: 12-27 kHz. Top: red dotted lines show the bounds (two times the standard deviation) around the average TS measurements obtained from 186 echoes within 0.30 degrees of the centre of the beam.

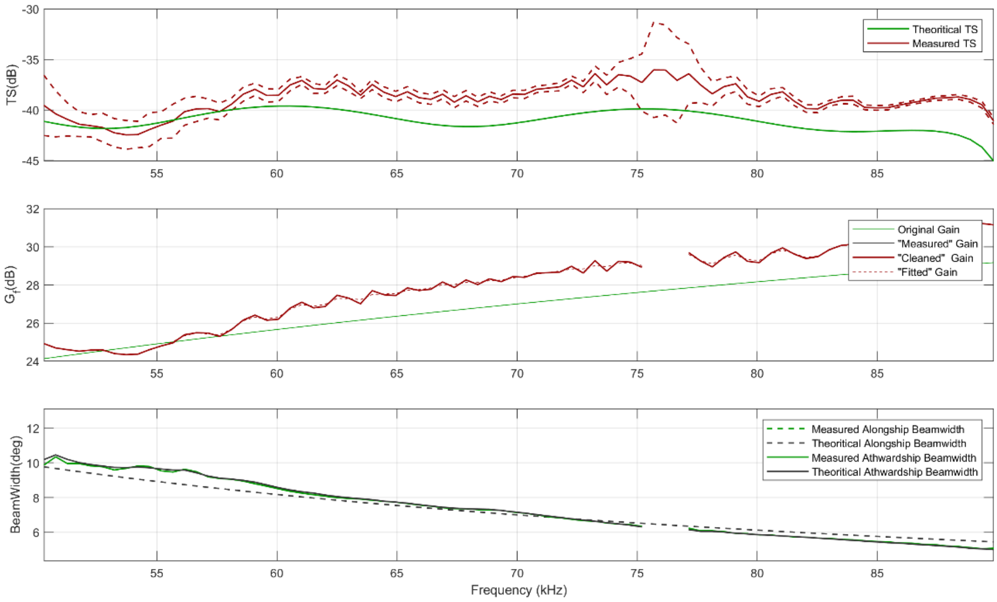

Figure A1. 13: Target strength (in dB re 1 m^2), gain, and beam angle estimation as a function of frequency for the 70 kHz WBT (50-90 kHz) for the calibration using a pulse length of 2.048 ms. Final usable bandwidth: 50-90 kHz. Top: red dotted lines show the bounds (two times the standard deviation) around the average TS measurements obtained from 45 echoes within 0.21 degrees of the centre of the beam.

Calibration report dual frequency towed body (DuFT)

Calibration of the Simrad EK80 echosounders in the dual frequency towed body (DuFT) took place on 28 August 2022 north of Banks Peninsula (43˚ 12.35’ S, 172˚ 01.63’ E), at the start of the acoustic survey of southern blue whiting stock on Campbell Island (TAN22101). The calibrations were conducted broadly as per the procedures of Demer et al. (2015). The wideband transceiver (WBT) tube on the DuFT runs the 38 and 120 kHz echosounders, with the 120 kHz being a broadband system. We calibrated the 120 kHz echosounder in narrowband at its nominal central frequency (i.e., 120 kHz) and broadband for a bandwidth of 90–160 kHz.

The DuFT was lowered about 5 m below the surface, supported by the deployment wires and a nose rope to allow the pitch to be adjusted. A 38.1 mm tungsten carbide sphere was suspended by a single line about 11 m below the transducer. A weight was also deployed about 6 m below the sphere to steady the line. The transducer face, DuFT window, sphere, and associated lines were washed with a soap solution prior to entering the water.

The weather during the calibration was good with 10 knots of south-easterly wind and 1 m swell. The vessel was allowed to drift (‘unclutched’) but, due to the direction of the drift, the position of the vessel was adjusted using one of the thrusters. The calibration started at 9:11 and was completed at 10:42 NZST.

The echosounder was run from inside the DuFT and calibration data were saved into Simrad EK80 raw format files: D20220827-T211136, D20220827-T221956, and D20220827-T224217. These data are stored in the NIWA *acoustics* database. The EK60 transceiver settings in effect during the calibration are given in Table A1. 4.

A temperature/salinity/depth profile was taken using a Seabird SBE37-SM (V 2.6b Serial No. 2958) conductivity, temperature, and depth probe (CTD). Estimates of acoustic absorption were calculated using the formulae of Doonan et al. (2003). The formula from Francois & Garrison (1982) was used at 200 kHz. Estimates of seawater sound speed and density were calculated using the formulae of Fofonoff & Millard (1983). The sphere target strength was calculated as per equations 6 to 9 of MacLennan (1981), using longitudinal and transverse sphere sound velocities of 6853 and 4171 m s^{-1} respectively and a sphere density of 14 900 kg m^{-3}.

The DuFT was lowered about 3 m below the surface, supported by the deployment wires and a nose rope to allow the pitch to be adjusted. A 38.1 mm tungsten carbide sphere was suspended by a single line about 35 m below the transducer. A weight was also deployed about 3 m below the sphere to steady the line. The transducer face, DuFT window, sphere, and associated lines were washed with a soap solution prior to entering the water.

Analysis

The data in the .raw files were extracted using custom-written ESP3 software (version 1.46.4). The amplitude of the sphere echoes was obtained by filtering on range and choosing the sample with the highest amplitude. Instances where the sphere echo was disturbed by fish echoes were discarded. The alongship and athwartship beam widths and offsets were calculated by fitting the sphere echo amplitudes to the Simrad theoretical beam pattern:

$$compensation = 6.0206\left(\left(\frac{2\theta_{fa}}{BW_{fa}}\right)^2 + \left(\frac{2\theta_{ps}}{BW_{ps}}\right)^2 - 0.18\left(\frac{2\theta_{fa}}{BW_{fa}}\right)^2\left(\frac{2\theta_{ps}}{BW_{ps}}\right)^2\right),$$

where θ_{ps} is the port/starboard echo angle, θ_{fa} the fore/aft echo angle, BW_{ps} the port/starboard beamwidth, BW_{fa} the fore/aft beamwidth, and *compensation* the value, in dB, to add to an uncompensated echo to yield the compensated echo value. The fitting was done using an unconstrained nonlinear optimisation (as implemented by the Matlab `fminsearch` function). The S_a correction was calculated from:

$$Sa, corr = 5\log 10\left(\frac{\sum P_i}{4P_{\max}}\right),$$

where P_i is sphere echo power measurements and P_{max} the maximum sphere echo power measurement. A value for $S_{a,corr}$ is calculated for all valid sphere echoes and the mean over all sphere echoes is used to determine the final $S_{a,corr}$.

Results

The results from the CTD casts are given in Table A1. 5, along with estimates of the sphere target strength, sound speed, and acoustic absorption.

The calibration results for both channels are given in Table A1. 6. The estimated beam pattern and sphere coverage are given in Figures A1. 14–15 for the 38 kHz and Figures A1. 16–17for the 120 kHz. The symmetrical nature of the pattern and the zero centre of the beam pattern indicate that the transducers and WBT-Tube channels were operating correctly. The RMS of the difference between the Simrad beam model and the sphere echoes the sphere echoes out to 3dB of the centre was 0.18 dB for the 38Hz and 0.25dB for the 120 Hz (where <0.2 dB excellent 0.2–0.3 dB good and <0.4dB acceptable).

Results of the broadband calibration showed a change of beamwidth with frequency that matched the theoretical curves (see Figure A1. 18). The gain for the 120 kHz WBT showed strong changes over the bandwidth, which was expected given the narrow band of the transducer used. The consistency of TS measurement (see bounds in Figure A1. 18) showed a consistent behaviour of the transducer in the 90–160 kHz frequency band.

References

Demer, D.A.; Berger, L.; Bernasconi, M.; Bethke, E.; Boswell, K.; Chu, D.; Domokos, R.; et al. (2015). Calibration of acoustic instruments. *ICES Cooperative Research Report No. 326*. 133 p.

Doonan, I.; Coombs, R.; McClatchie, S. (2003). The absorption of sound in seawater in relation to estimation of deep-water fish biomass. *ICES Journal of Marine Science 60*: 1047–1055.

Fofonoff, P.; Millard, R., Jr (1983). Algorithms for computation of fundamental properties of seawater. *UNESCO Technical Papers in Marine Science 44*. 53 p.

MacLennan, D.N. (1981). The theory of solid spheres as sonar calibration targets. *Scottish Fisheries Research 22*. 17 p.

Table A1. 4: EK80 transceiver settings and other relevant parameters in effect during the calibration.

Parameter		
Frequency (kHz)	38	120
WBT model	WBT-Tube	WBT-Tube
WBT serial number	253657	253688
GPT/WBT software version	1.01	1.01
EK80 software version	21.15.1	21.15.1
Transducer model	ES38DD	ES120-7CD
Transducer serial number	666	124
Sphere type/size	tungsten carbide /38.1 mm	tungsten carbide / 38.1 mm
Transducer draft setting (m)	0.0	0.0
Transmit power (W)	1000	250
Pulse length (ms) CW	1.024	1.024
Transducer peak gain by pulse length (dB)	25.5	27.0
Sa correction (dB)	0.00	0.00
Bandwidth (Hz)	0	0
Sample interval (ms) by pulse length (dB)	0.04	0.04
Two-way (equivalent) beam angle (dB)	–20.7	–20.7
Angle sensitivity (dB) along/athwartship	23.0/23.0	23.0/23.0
3 dB beamwidth (º) along/athwartship	7.0/7.0	7.0/7.0
Angle offset (º) along/athwartship	0.0/0.0	0.0/0.0

Table A1. 5: CTD cast details and derived water properties. The values for sound speed, salinity, and absorption are the mean over water depths 6 to 30 m.

Parameter	
Date/time (NZST, start)	28 August 2022 17:45
Position	43˚ 12.35’ S, 172˚ 01.63’ E
Mean sphere range (m)	13.9 (38Hz), 13.7 (120z)
Mean temperature (ºC)	9.9
Mean salinity (psu)	34.0
Sound speed (m/s)	1489.2
Water density (kg/m^3)	1026.7
Sound absorption (dB/km)	9.89 (38 kHz) 36.87 (120 kHz)
Sphere target strength (dB re 1m^2)	–42.39 (38 kHz) –39.48 (120 kHz)

Table A1. 6: Echosounder calibration values for all calibrations of EK80 echosounder on the DuFT. Transducer peak gain was estimated from mean sphere TS.

		Aug 2022	June 2021
38 kHz			
	Transducer peak gain (dB)	24.34	24.65
	Sa correction (dB)	-0.04	-0.15
	Beamwidth (º) along/athwartship	6.6/6.7	6.8/4.6
	Beam offset (º) along/athwartship	0.07/0.00	-0.02/-0.03
	RMS deviation (dB)	0.18	0.18
120 kHz			
	Transducer peak gain (dB)	27.05	27.44
	Sa correction (dB)	-0.13	-0.11
	Beamwidth (º) along/athwartship	6.7/6.9	7.15/7.13
	Beam offset (º) along/athwartship	-0.01/-0.08	0.06/-0.06
	RMS deviation (dB)	0.25	0.17

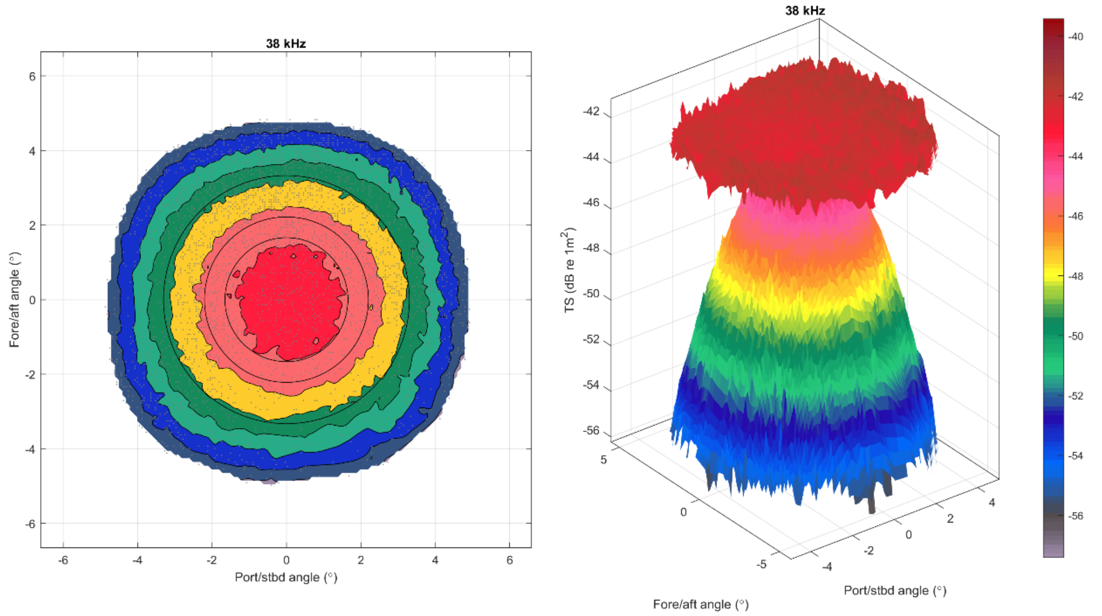

Figure A1. 14: The 38 kHz estimated beam pattern from the sphere echo strength and position. The '+' symbols indicate where sphere echoes were received. The colours indicate the received sphere echo strength in dB re 1 m^2.

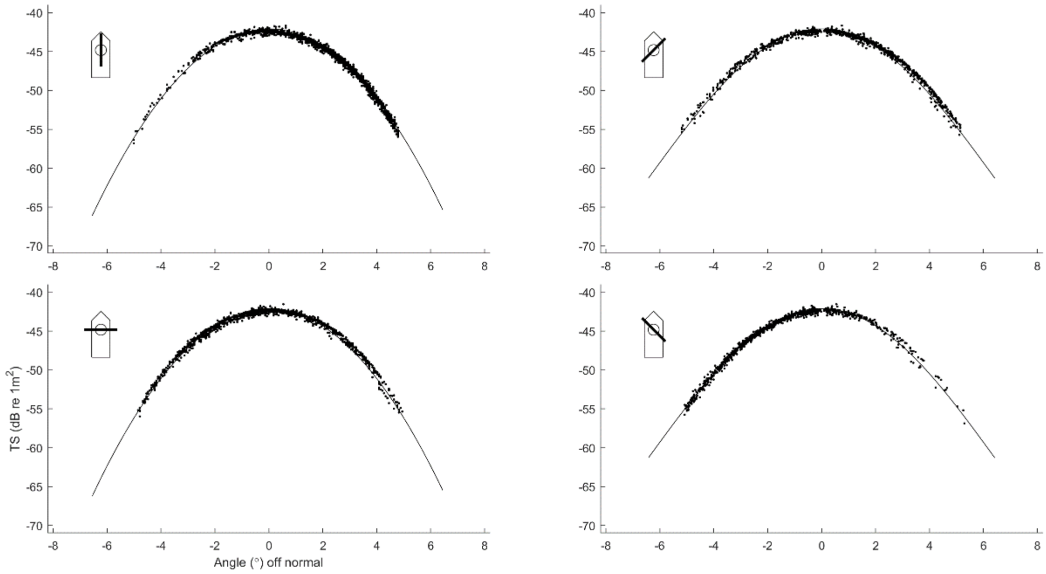

Figure A1. 15: 38 kHz beam pattern results from the calibration analysis. The solid line is the theoretical beam pattern fit to the sphere echoes for four slices through the beam.

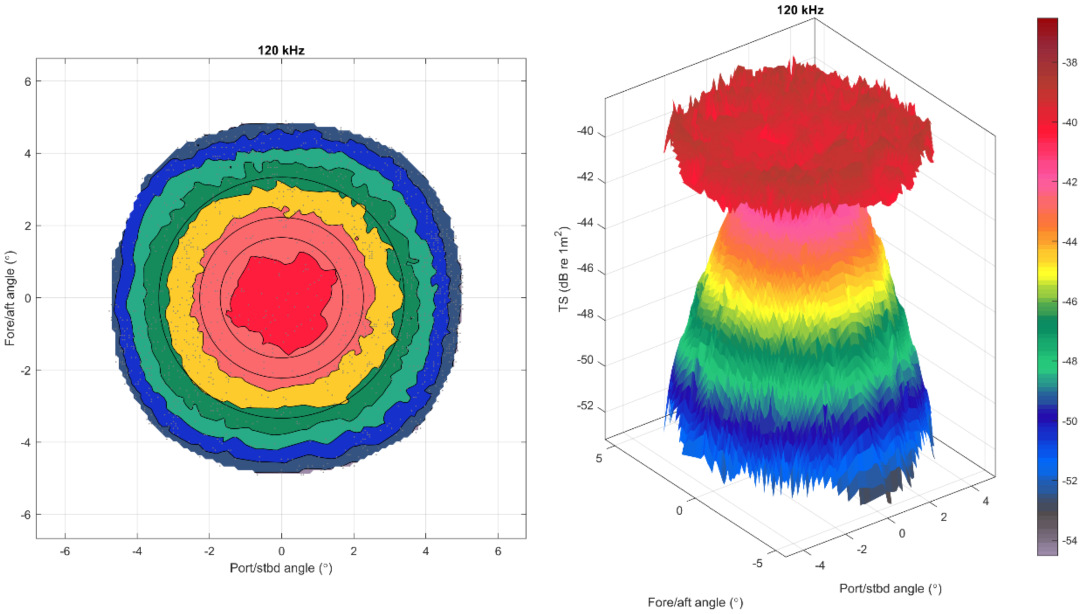

Figure A1. 16: The 120 kHz estimated beam pattern from the sphere echo strength and position. The '+' symbols indicate where sphere echoes were received. The colours indicate the received sphere echo strength in dB re 1 m^2.

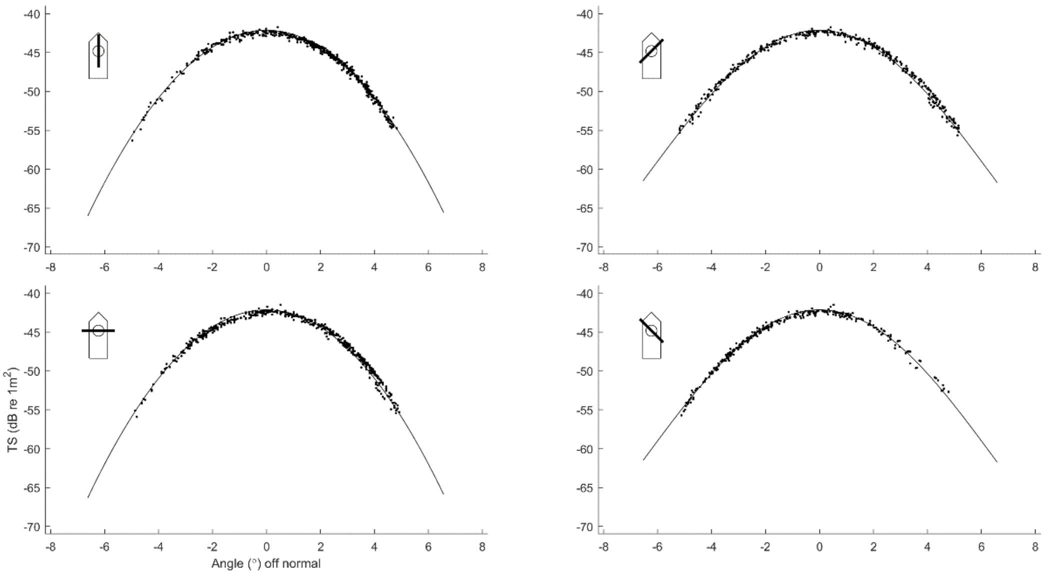

Figure A1. 17: 120 kHz beam pattern results from the calibration analysis. The solid line is the theoretical beam pattern fit to the sphere echoes for four slices through the beam.

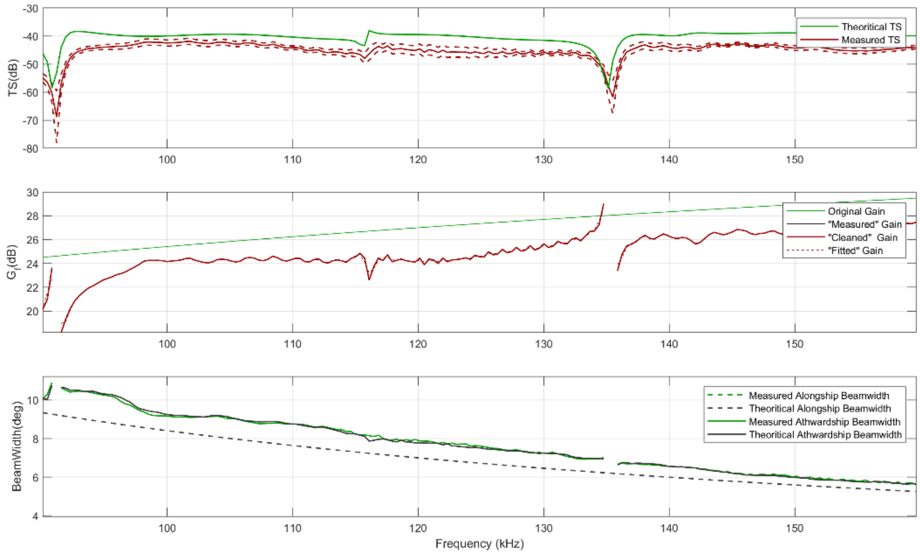

Figure A1. 18: Target strength (in dB re 1 m^{-2}), gain, and beam angle estimation as a function of frequency for the 120 kHz WBT (90-160 kHz) for the calibration done using a pulse length of 2.048 ms. Final usable bandwidth: 90-160 kHz. Top: red dotted lines show the bounds (two times the standard deviation) around the average TS measurements obtained from 186 echoes within 1.05 degrees of the centre of the beam.

APPENDIX 2: Calculation of sound absorption coefficients and sound speed

The temperature and salinity data collected using a Seabird SM-37 Microcat CTD datalogger (serial number 2958) mounted on the headline of the demersal trawl net, and temperature data collected with an RBR data logger (RBR*duet*, serial number 82704) attached on the midwater trawls, were used calculate the absorption coefficient and speed of sound, and to define water mass characteristics in the area.

The water column was mixed with no clear stratification (see Figure A2. 1). Average sound absorption was estimated using the formula of Doonan et al. (2003) and the average sound speed using the formula of Fofonoff & Millard (1983) (Table A2. 1).

The average absorption estimates of 9.40 dB km^{-1} was used to process acoustic data collected during the 2022 Campbell Island acoustic survey.

Table A2. 1: Estimates of acoustic absorption (at 38 kHz) for the Campbell Island Rise acoustic survey area in 2022.

Station	Mean temperature (°C)	Mean salinity (PSU)	Max. depth (m)	Absorption (dB/km)	Mean sound speed (m/s)
1	7.52	34.37	525.25	9.27	1 484.72
2	7.47	34.37	360.32	9.43	1 482.97
3	7.42	34.37	499.99	9.31	1 484.05
4	7.34	34.37	344.70	9.46	1 482.36
5	7.40	34.38	375.48	9.43	1 482.89
*6	7.68	NA	474.22	NA	NA
*7	7.66	NA	551.47	NA	NA
8	7.36	34.37	409.03	9.40	1 483.05
9	7.36	34.37	367.87	9.44	1 482.66
*10	7.35	NA	394.03	NA	NA
11	7.40	34.39	354.63	9.45	1 482.69
*12			No data collected - RBR failed		
Mean	7.45	34.37	423.36	9.40	1 483.18

* Midwater trawls where RBR was used therefore no salinity data.

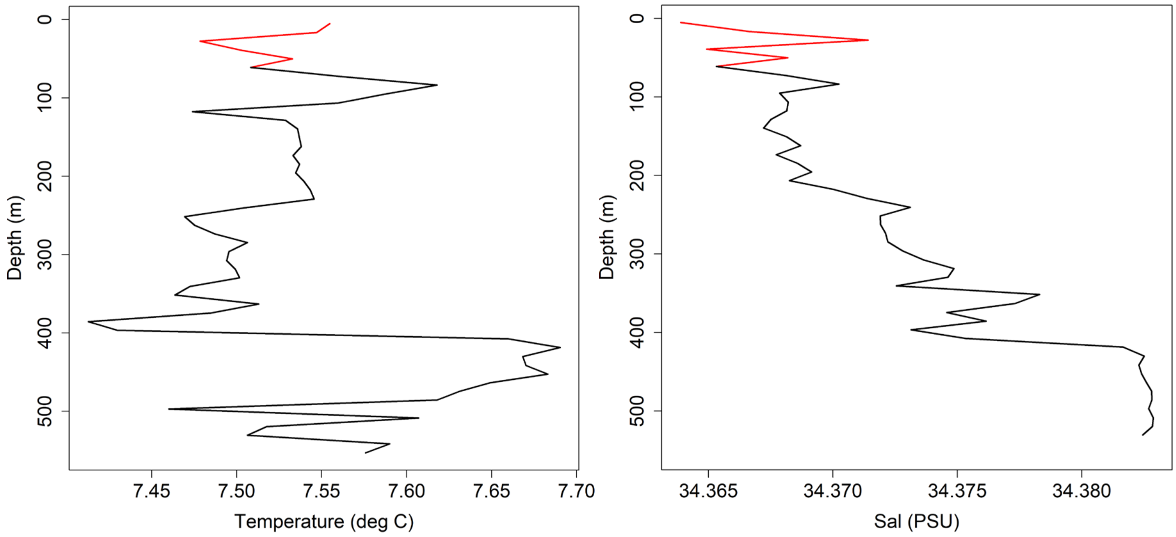

Figure A2. 1: Vertical profiles of average temperature (left) and salinity (right), calculated in ten-metre vertical bins for the Campbell Island Rise during the 2022 southern blue whiting acoustic survey. Red and black lines indicate depth range above and below the average depth of dual frequency towed body. Temperature and salinity data were collected using a Seabird SM-37 Microcat CTD datalogger in all demersal trawls (n = 7). Temperature data were also collected using an RBR*duet* data logger in four midwater trawls (n = 4).

APPENDIX 3: Description of gonad development used for staging southern blue whiting

Research gonad stage		Males	Females
1	Immature	Testes small and translucent, threadlike or narrow membranes.	Ovaries small and translucent. No developing oocytes.
2	Resting	Testes thin and flabby; white or transparent.	Ovaries are developed, but no developing eggs are visible.
3	Ripening	Testes firm and well developed, but no milt is present.	Ovaries contain visible developing eggs, but no hyaline eggs present.
4	Ripe	Testes large, well developed; milt is present and flows when testis is cut, but not when body is squeezed.	Some or all eggs are hyaline, but eggs are not extruded when body is squeezed.
5	Running-ripe	Testis is large, well formed; milt flows easily under pressure on the body.	Eggs flow freely from the ovary when it is cut or the body is pressed.
6	Partially spent	Testis somewhat flabby and may be slightly bloodshot, but milt still flows freely under pressure on the body.	Ovary partially deflated, often bloodshot. Some hyaline and ovulated eggs present and flowing from a cut ovary or when the body is squeezed.
7	Spent	Testis is flabby and bloodshot. No milt in most of testis, but there may be some remaining near the lumen. Milt not easily expressed even when present.	Ovary bloodshot; ovary wall may appear thick and white. Some residual ovulated eggs may still remain but will not flow when body is squeezed.